BABAR Analysis Document 1390
Version 5
August 13, 2006

A search for $B^+ \to K^+\nu\overline{\nu}$ using hadronic B^- tags

Joachim Harnois-Deraps, Steven Robertson
McGill University

Abstract

The document describes a search for the rare decay $B^+ \to K^+\nu\overline{\nu}$ in a data set of $208.73\,\mathrm{fb}^{-1}$ collected at the $\Upsilon(4S)$ resonance by the *BABAR* detector. Signal candidate events are selected by identifying the highest momentum $K^{\pm}$ recoiling against a tag B^- that has decayed hadronically, using the semi-exclusive reconstruction method. The number of signal events candidate observed is ???±???±???, while 14.95 ± 1.75 (stat) ± 1.09 (syst) background events are expected from a blind analysis technique. We set an upper limit of $\mathcal{B}(B^+ \to K^+\nu\overline{\nu}) <???? \times 10^{-5}$, at the 90% confidence level.

Contents

1 Introduction

1.1 Flavor Changing Neutral Currents

The Standard Model of particle physics (SM) has proven to be very close to nature in a wide range of experiments, but is expected to fail at very high energies. Physicists created new models that could possibly explain and describe the expected discrepancy, either by adding compact extra dimensions [1], a 4th generation of leptons or quarks with various interactions [2] [3] [4], charged Higgs bosons [5], right-handed fermions [6], lepton number violating modes [7] or various supersymmetric partners [8], just to name a few.

Some interaction could be extremely sensitive to these new physics scenarios, especially those involving flavor-changing neutral currents (FCNC), like $b \to (s/d)\gamma$, $b \to (s/d)\ell^+\ell^-$, $b \to (s/d)\nu\overline{\nu}$, $c \to u\ell^+\ell^-$, $c \to u\nu\overline{\nu}$ and $s \to d\nu\overline{\nu}$. These decays are forbidden at the tree-level by the SM, but can occur at the loop-level, like in penguin or box diagrams (see diagrams below). Possible tree-level interactions are observed to be heavily suppressed by experiments [**?**]. New interactions could occur within the loop, and the Branching ratios of these decays could be enhanced significantly.

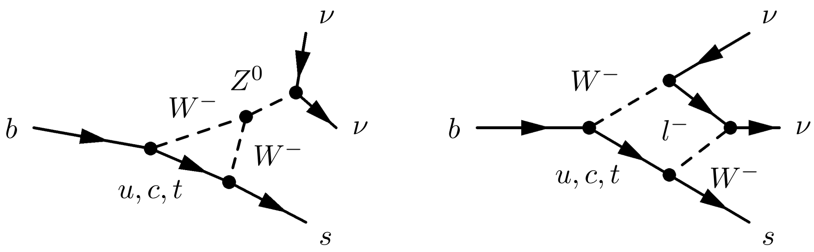

Penguin (left) and Box (right) Feynman diagrams for the process $b \to (s/d)\nu\overline{\nu}$, as predicted by the SM. In both cases the amplitudes are expected to be dominated by the heavy t quark contribution. Many New Physics scenarios could contribute to this process, modifying slightly these two diagrams.

In nature, quarks are confined to hadrons, so the decay of the b quark occurs usually within a B meson, which is a two body bound state. Meson wave functions are not well known, but we can avoid the related theoretical uncertainty by studying inclusive decays $B \to X_{d,s}\nu\overline{\nu}$, in which a *spectator* quark, originally accompanying the b quark, combines with the final q quark in any meson $X_{s,d}$. The branching ratios are predicted to be $\mathcal{B}(B \to X_s\nu\overline{\nu}) = (4.1^{+0.8}_{-1.0}) \times 10^{-5}$, and $\mathcal{B}(B \to X_d\nu\overline{\nu}) = 3.5 \times 10^{-5}$[9]. There is currently no experimental upper limit on the X_d processes, but for the X_s processes, an upper limit of $\mathcal{B}(B \to X_s\nu\overline{\nu}) < 6.4 \times 10^{-4}$ is set by the ALEPH collaboration [10].

1.2 Finding $\mathcal{B}(B^+ \to K^+\nu\overline{\nu})$

In a B Factory, it is hard to search for inclusive processes like $b \to (s/d)\nu\overline{\nu}$ due to the undetected energy of two neutrinos, which makes it impossible to fully reconstruct the decaying B meson, and which also limits the power to reject other B decays that fake the signal process. However, some exclusive mode like $B^+ \to K^+\nu\overline{\nu}$ [1] have less precise theoritical predictions, but are much easier to reconstruct. This particular mode is predicted to compose about 9% of the $b \to s\nu\overline{\nu}$ inclusive rate, and kaons are well detected and identified by the *BABAR* detector, so $B^+ \to K^+\nu\overline{\nu}$ is a good candidate for a search of FCNC process. According to the SM, $B^+ \to K^{*+}\nu\overline{\nu}$ is predicted to have $\mathcal{B}(B^+ \to K^{*+}\nu\overline{\nu}) < (1.3^{+0.4}_{-0.3}) \times 10^{-5}$, which composes about 32% of the inclusive rate, and these numbers are conserved in the decays $B^0 \to K^{(*)0}\nu\overline{\nu}$. However, reconstructing a K^* candidate has its own challenge, and is left for a future analysis.

The decay rate of a $B^\pm$ meson with momentum p_B into a Kaon of momentum p_K contains the matrix element [11]

$$\langle K(p_K) \mid \overline{s}\gamma_\mu b \mid B(p_B)\rangle = f_+(q^2)(p_B + p_K)_\mu + f_-(q^2)q_\mu \tag{1}$$

where $f_\pm$ are model dependent form factors and $q_\mu = (p_B - p_K)_\mu$. In the SM, assuming that there are no right-handed neutrinos, the Wilson coefficient C_L^ν is computed with the method of effective Hamiltonian [13], and the decay rate is given by [11]

$$\frac{d\Gamma}{ds}(B^+ \to K^+\nu\overline{\nu}) = \frac{G_f^2\alpha^2 m_B^5}{256\pi^5}|V_{ts}V_{tb}|^2\lambda_K^{3/2}(s)f_+^2(s)|C_L^\nu|^2 \tag{2}$$

where $\sqrt{s}$ is the center-of-mass energy, m_B the B meson mass, G_f the Fermi constant, α the fine structure constant and $\lambda_K(s) = 1+(\frac{m_K}{m_B})^4+s^2-2s-2(1+s)(\frac{m_K}{m_B})^2$. The form factors are found here in the "Godfrey Isgur" model [14] with a switched-off one-gluon exchange, in very good agreement with latice QCD at high q^2, and it prescribes

$$f_+(s) = \frac{f_+(0)}{1-\sigma_1 s + \sigma_2 s^2}, \qquad (f_+(0), \sigma_1, \sigma_2) = (0.33, 0.0519, 0.00065) \tag{3}$$

where $f_+(0)$, σ_1 and σ_2 the parameters of the model. The branching fraction is predicted to be $\mathcal{B}(B^+ \to K^+\nu\overline{\nu}) = (3.8^{+1.2}_{-0.6}) \times 10^{-6}$ [11], with the error coming from the uncertainty in the form factors.

An experimental measurement of $B^+ \to K^+\nu\overline{\nu}$ can not be differentiated from a measurement of $B^\pm \to K^\pm SS$, in which S is a cold dark matter scalar [12]. The neutrinos and the scalars do not interact with the *BABAR* detector, so the events look like $B^\pm \to K^\pm +$ *missing energy*. However, the SM expectation for the neutrino case is known with a better accuracy, so the measurement can put restrictions on parameters of the scalar process.

With the high luminosity produced at PEP-II, *BABAR* has a few hundreds of millions of B mesons which allow studies at the level of expectation for exclusive modes like $B^+ \to K^{(*)+}\nu\overline{\nu}$ or $B^+ \to \pi^+\nu\overline{\nu}$. The present analysis focus exclusively on $B^+ \to K^+\nu\overline{\nu}$ process. It uses the semi-exclusive method with hadronic tag to reconstruct one of the B meson and look in the rest of the event for the signal process.

Criteria imposed on the reconstructed B candidates are discussed in section 3, while the search for the signal process is analyzed in section 4. Background estimates and sidebands will be described in sections 6 and 7 respectively, the study of systematic errors in sections 9 and the physics results are found in section 8.

[1] Charge conjugate modes are implied throughout this paper

2 Samples and Lists

This section describes the data and the Monte Carlo samples used in this analysis. Both types of events are filtered with the `BSemiExcl` reconstruction skim and are accessed from the database by the `BbkDataSetTcl` utility.

2.1 Data Sample

This analysis uses $208.73\,\mathrm{fb}^{-1}$ of "onpeak" data taken at the $\Upsilon(4S)$ resonance and $21.49\ \mathrm{fb}^{-1}$ of "offpeak" data recorded at 40 MeV below onpeak to study non-resonnant backgrounds. These luminosities correspond to *BABAR* Run1 to Run4.

The recorded events pass at least one drift chamber (DCH) and one electromagnetic calorimeter (EMC) trigger requirements, as well as the `BGFMultiHadron` filter. The latter requires that there is at least three charged tracks in the detector, and to suppress most QED background like $e^+e^- \to \ell^+\ell^-(\gamma)$, it also rejects events with R2 of all tracks and clusters greater 0.5, where R2 is the ratio of the zeroth to the second Fox-Wolfram moment [16]. These requirements are listed in table 2.

Table 1: Cross-sections used in this analysis, at the $\Upsilon(4S)$ resonance.

type	σ (nb)
$e^+e^- \to b\bar{b}$	1.05
$e^+e^- \to c\bar{c}$	1.30
$e^+e^- \to s\bar{s}$	0.35
$e^+e^- \to u\bar{u}$	1.39
$e^+e^- \to d\bar{d}$	0.35
$e^+e^- \to \tau^+\tau^-$	0.94

Table 2: Filters used in the skimming process.

Filters	Requirements
L3 DCH 1	$N_{\mathrm{trk}} \geq 1$, $p_t > 600\,\mathrm{MeV}/c$, $DOCA - XY < 1.0$ cm , $DOCA - Z < 7.0$ cm
L3 DCH 2	$N_{\mathrm{trk}} \geq 2$, $p_t > 250\,\mathrm{MeV}/c$, $DOCA - XY < 1.5$ cm , $DOCA - Z < 10.0$ cm
L3 EMC 1	$N_{\mathrm{clus}} \geq 2$, $E^* > 350\,\mathrm{MeV}$, event mass $> 1.5\,\mathrm{GeV}$
L3 EMC 2	$N_{\mathrm{clus}} \geq 4$, $E^* > 350\,\mathrm{MeV}$, event mass $> 1.5\,\mathrm{GeV}$
`BGFMultiHadron`	$N_{\mathrm{trk}} \geq 3$, R2 of all tracks and clusters < 0.5

2.2 Generic Monte Carlo Samples

In order to study the different types of background events, we use all the skimmed SP5/6 generic Monte Carlo (MC) samples of B^+B^-, $B^0\overline{B}^0$, $c\bar{c}$, uds and $\tau^+\tau^-$ available at the time. Runs 1-3 are modeled by SP5, and Run4 by SP6 simulation productions. The `BGFMultiHadron` filter, one L3 trigger requirement on the DCH and one on the EMC were imposed as part of the `BSemiExcl` reconstruction procedure. The sizes of each samples used in this analysis are listed in Table 3, both in number of events and in luminosity. The equivalent luminosity assumes the cross sections of Table 1.

Table 3: Data and generic Monte Carlo samples used in this analysis

Decay	SP5/6 mode #	Number of events	Equivalent Lumi (fb^{-1})
$B^+B^- \to$ anything	1235	584 026 k	1112.43
$B^0\overline{B}^0 \to$ anything	1237	540 742 k	1029.98
$c\overline{c} \to$ anything	1005	425 792 k	327.53
$uds \to$ anything	998	677 217 k	324.03
$\tau^+\tau^- \to$ anything	3429	346 636 k	368.76
Onpeak data	Runs 1-4	1 888 340 k	208.73 fb^{-1}
Offpeak data	Runs 1-4	284 114 k	21.49 fb^{-1}

2.3 Signal Monte Carlo Samples

Finally, this analysis has 285 000 skimmed $B^+ \to K^+\nu\overline{\nu}$ signal events at its disposal, simulated with a phase space model, in which one B^+ decays into the signal channel while the companion B^- decays generically. Because of the low reconstruction efficiency of the semi-exclusive method, we also use "cocktail" MC signal events, in which the B^- decays in very clean modes ; the reconstruction efficiency is enhanced and it increases the statistics of some distributions.

The estimation of the reconstruction efficiency can be improved by combining the statistics of the signal channel with that of modes topologically similar, like $B^+ \to K^{*+}\nu\overline{\nu}$ and $B^+ \to \pi^+\nu\overline{\nu}$. These two modes can potentially fake the $B^+ \to K^+\nu\overline{\nu}$ signal, so they are used to estimate the number background events coming from $K^{*\pm}$ and $\pi^\pm$ modes exclusively. For that sake, we assume Branching Fraction ($\mathcal{B}$) corresponding to the last experimental Upper limit (UL) from *BABAR* on each modes.

There is currently no upper limit on the the K^* mode, so we assume that the experimental resolution on this mode is at the same "distance" from its SM prediction as in the case of the $B^+ \to K^+\nu\overline{\nu}$ mode.

Details on the signal MC samples used in this analysis are found in Table 4.

2.4 Lists of Particles

We are running our analysis on `R16a BSemiExcl` skimmed events. These are analyzed in release 16.1.5 with the `BRecoilTools` and `BRecoilUser` packages "out of the box", using `chargedTracks` and `calorNeutral` as input lists for charged and neutral particles respectively. Tracks are assigned the $\pi^\pm$ mass by hypothesis, unless they satisfy the likelihood tight kaon criteria, in which case they are assigned the $K^\pm$ mass and added to the `KLHTight` list. K^0_S are reconstructed from $K^0_S \to \pi^+\pi^-$ with a K^0_S mass constraint imposed, and intermediate K^0_S states are accepted with a displaced vertex.

Two clusters are combined to form a loose π^0 candidate if their invariant mass is in the interval 0.115 - 0.150 GeV/c^2. However, the clusters used in the π^0 reconstruction are not removed from

Table 4: Modes, number of events and upper limits of signal Monte Carlo used in this analysis. The *BABAR* analysis that sets the UL on the $\pi^{\pm}$ mode used hadronic tags only, while the limit on the $K^{\pm}$ channel was found using both hadronic and semi-leptonic tags [17]. Both used 82 fb^{-1} of onpeak data, corresponding to *BABAR* Run1-2.

Signal	SP5/6 mode #	Number of events	Upper Limits at 90% Confidence Level
$B^+ \to K^+\nu\overline{\nu}$ vs generic B	2227	285 000	$\mathcal{B}(B^+ \to K^+\nu\overline{\nu}) = 5.2 \times 10^{-5}$
$B^+ \to K^+\nu\overline{\nu}$ vs $B^- \to D^{(*)0}\pi^-$	2574	127 000	-
$B^+ \to K^+\nu\overline{\nu}$ vs $B^- \to D^{(*)0}\rho/a_1$	2674	123 000	-
$B^+ \to K^{*+}\nu\overline{\nu}$ vs generic B	3656	235 000	$\mathcal{B}(B^+ \to K^{*+}\nu\overline{\nu}) = 1.77 \times 10^{-4}$
$B^+ \to \pi^+\nu\overline{\nu}$ vs generic B	3346	57 000	$\mathcal{B}(B^+ \to \pi^+\nu\overline{\nu}) = 1.0 \times 10^{-4}$

the `calorNeutral` list, so we must be careful when dealing with π^0 and clusters to avoid double-counting.

These intermediate states were combined with the `SimpleComposition` tool. A summary of packages and particle lists used is shown in Table 5.

Table 5: Tags and particle lists used in this analysis

BRecoilUser	V00-03-01
BRecoilTools	V00-05-03
workdir	V00-04-20
Cluster list	`calorNeutral`
Track list	`chargedTracks`
$K^{\pm}$ list	`KLHTight`
π^0 list	`pi0Loose`
K^0_S list	`KsDefault`

3 B_{tag} Selection

For each event, the `BSemiExcl` package reconstruct the best B meson by looking for specific decay modes. It is possible to select a subset of these in order to reject low purity modes and reduce the systematic error, but in this analysis we choose to keep all modes and maximize the statistics. Anyway, an *a priori* purity cut is imposed by the `BSemiExcl` skim. Events in which a B candidate satisfy the B_{tag} selection are tagged, as they create good conditions to observe the signal process. In this section, we describe the reconstruction of B mesons, the selection of the B_{tag}, and the method to extract the tagging yield and efficiency.

3.1 Semi-Exclusive Method

The process $B^+ \to K^+ \nu\overline{\nu}$ is a three body decay in which 2 particles are undetected. The neutrino system can carry an amount of energy ranging from almost nothing to more than 4 GeV, so the momentum of the kaon has a broad spectrum. In a B Factory environment, where two B mesons decay in the detector, this topology is very hard to constrain kinematically. We are looking for a hard K^+ recoiling against the decay product of the B^- companion.

The semi-exclusive method consists in reconstructing one of the B meson (tag side) and to search for the signal channel in the rest if the event (signal side). In order to clean up the signal side of the event, the reconstructed B candidate is required to decay hadronically in one of the allowed high-purity modes. In the signal side, the tracks and clusters come primarily from the decay of the unreconstructed B, called B_{sig}. This method is a good compromise between suppressing a lot of QED and continuum events while keeping a reasonable B reconstruction efficiency.

3.2 Reconstructing the Best B

The procedure used in the `BSemiExcl` skim to reconstruct the $B^+ \to D^{(*)0} X^+$ process is summarized here for completeness, but is detailed elsewhere [18]. D^0 candidates are reconstructed via the decays $D^0 \to K^-\pi^+$, $D^0 \to K^-\pi^+\pi^0$, $D^0 \to K^-\pi^+\pi^+\pi^-$ or $D^0 \to K^0_S\pi^+\pi^-$, and can be combined with a γ or a π^0 to produce a D^* candidate. Appart from K^0_S and π^0, no other intermediate states are reconstructed. We start with a $D^{(*)0}$ "seed" and add pions and kaons one at a time. Each possible combination for this X^+ system is considered, but good candidates must have an energy E^*_B close to the beam energy $E^*_{\rm beam}$, and the beam-energy substituted $m_{\rm ES}$ mass has to be close to the nominal m_B. Namely, it keeps candidates with

$$-0.2\,\text{GeV} < \Delta E < 0.2\,\text{GeV}, 5.220 < m_{\rm ES} < 5.230\,\text{GeV}/c^2 \tag{4}$$

where $\Delta E = E^*_B - E^*_{\rm beam}$ and $m_{\rm ES} = \sqrt{{E^*_{\rm beam}}^2 - p^*_B}$. p^*_B is the momentum of the candidate B meson in the center-of-mass (CM) frame. In a perfect detector environment and with a perfect reconstruction algorithm, the $m_{\rm ES}$ for a signal event would be a delta function centered at the nominal B mass m_B. However, there is a spread of a few MeV coming from $E^*_{\rm beam}$, and the reconstruction algorithm can mis-reconstruct an event and exclude tracks that originate from the selected B, decreasing significantly the value of $m_{\rm ES}$.

The algorithm can combine up to 5 ($\pi^\pm$ + $K^\pm$), up to 2 π^0 and 1 K^0_S (see Table 6). If more than one B candidates are reconstructed, the B with the smallest ΔE is chosen. The $m_{\rm ES}$ variable is thus unbiased by this selection and can be used to reject background events. B^0 candidates are simultaneously reconstructed using $D^{(*)+}$ seeds, so the selected B can be either neutral or charged.

3.3 Backgrounds

Unfortunately, the algorithm can reconstruct unphysical, or fake B mesons candidates. These background events are classified in three categories :

1. *Continuum background* (i) No $\Upsilon(4S)$ is produced, the collision is a $e^+e^- \to \tau^+\tau^-$event, but hadrons produced in the decays of the lepton are randomly combined by the `BSemiExcl` algorithm into a B meson candidate. Only a small amount of these QED events pass the skim.

2. *Continuum background* (ii) No $\Upsilon(4S)$ is produced, the beam leptons annihilate and produce $u\overline{u}$, $d\overline{d}$, $s\overline{s}$ or $c\overline{c}$ quarks. These quarks decay into hadrons that are randomly combined to fake an allowed B decay mode. The initial quarks carry a lot of kinetic energy, hence they tend to produce events with back-to-back jets. In $c\overline{c}$ events, a $D^{(*)}$ seed may or may not be real, while for the three other quark types, grouped under the name "*uds*", the seeds are always unphysical.

3. *Combinatorial background* $\Upsilon(4S)$ is produced and decays into B^+B^- or $B^0\overline{B}^0$, however the best B candidate selected by the reconstruction algorithm is not the real meson, but a random combination of tracks and clusters, which happens to pass through the net.

The cross-sections for these processes are taken from the PDG [15] and listed in Table 1.

Table 6: Allowed hadronic decays of a B candidate. Charge conjugate processes are also reconstructed.

Reconstruction of intermediate states
$\pi^0 \to \gamma\gamma$
$K^0_S \to \pi^+\pi^-$
$D^0 \to K^-(\pi^+, \pi^+\pi^0, \pi^+\pi^+\pi^-)$
$D^0 \to K^0_S\pi^+\pi^-$
$D^{*0} \to D^0(\pi^0, \gamma)$
$B^+ \to D^{(*)0}X^+$
$X = a(K^\pm + \pi^\pm) + b\pi^0 + cK^0_S$ with a, b and $c \leq 5$, 2 and 2 respectively

3.4 Tag B Selection

Since the signal process we are looking for involves a charged B meson, the selected B candidates are required to have a charge Q_{tag} of ± 1. The Q_{tag} distribution is plotted in Figure 1 for skimmed events, and we observe that this first criteria rejects roughly a third of the background events. The m_{ES} distribution of the candidates is plotted in Figure 2 for all skimmed events, where offpeak data is scaled to the onpeak CM energy and luminosity.

We observe a slight shift in the peak central position, a known SP5/6 feature, but it has a negligible impact on the analysis if we choose a m_{ES} signal box large enough. For that purpose, we plot in Figure 3 the m_{ES} distribution for signal MC events with $Q_{\text{tag}} = \pm 1$, and we fit the distribution with a single gaussian. We do not assume that it models correctly the physics of the process, it is only used to define the signal box, a 3σ window around the mean, and a sideband, 4σ away from the mean.

Continuum events tend to be confined in back-to-back jets, so the distribution of θ_T, the angle between the momentum of the selected B_{tag} and the thrust axis (or sphericity axis) of all the signal side particles, has a strong peak at $\pm 180^o$. On the contrary, the decays of $B\overline{B}$ events produce a more isotropic distribution, so by rejecting events with $|\cos\theta_T|$ close to 1, we suppress a lot of these background events.

Figure 4 presents the $|\cos\theta_T|$ distribution for skimmed events with $Q_{\mathrm{tag}} = \pm 1$ and in the m_{ES} signal box. We observe a good agreement in the region $|\cos\theta_T| < 0.95$, for both onpeak and offpeak data. We apply a "loose" selection at $|\cos\theta_T| < 0.85$.

The three tagging selection requirements ("B_{tag} selection" criteria) are thus:

- $Q_{\mathrm{tag}} = \pm 1$
- $5.270 < m_{\mathrm{ES}} < 5.288\,\mathrm{GeV}/c^2$
- $|\cos\theta_T| < 0.85$

Skimmed events in which a reconstructed B candidate survives these three selection cuts are tagged, and we label such a candidate a "B_{tag}". We also define two sidebands to study continuum and/or combinatoric backgrounds :

- $5.225 < m_{\mathrm{ES}} < 5.265\,\mathrm{GeV}/c^2$
- $|\cos\theta_T| > 0.85$

Since the requirement on $\cos\theta_T$ is not really restrictive, we do not need a gap between the signal and the sideband criteria (i.e. by defining the sideband as $\cos\theta_T < 0.90$)

The m_{ES} distribution is shown in Fig. 5 for events that satisfy the two other tagging selection requirements. The Q_{tag} selector removes the "peak" in the signal region for simulated $B^0\overline{B}^0$ events; the $\cos\theta_T$ selector reduces the relative contribution from continuum background. There is still a good agreement between generic MC samples and onpeak data away from the peak, which suggests that continuum and combinatoric backgrounds are well modeled. The offpeak data are also in good agreement with simulated continuum background in the signal box, but do not match with MC in the sideband. This could be due to a higher reconstruction efficiency of `BSemiExcl` at a lower CM energy, and could be verified by comparing offpeak data to continuum MC background taken at offpeak CM energy. Unfortunately, these events are not skimmed at the moment, so the discrepancy cannot be investigated further.

Finally, we observe an excess of MC events in the peaking region, an effect that has a direct impact on the analysis and must be studied carefully. We can investigate this effect by studying the distribution of event shape variable in which different background types behave differently. For example, looking at variables like R2 (for all tracks and clusters) or at $\cos\theta_B$, the angle between the momentum of the B candidate and the beam pipe (Figures 6 and 7), we observe a good agreement between continuum and offpeak data, but a clear excess in generic B^+B^- MC events.

Since these events are well modeled in the m_{ES} sideband, we conclude that the excess comes mainly from the peaking component of the simulated B^+B^- events. This could be due to the uncertainty on the branching ratios of some B decays and on the `BSemiExcl` efficiency at reconstructing B candidates.

Table 7 shows the cumulative effect of the 3 B_{tag} requirements applied on MC and data events.

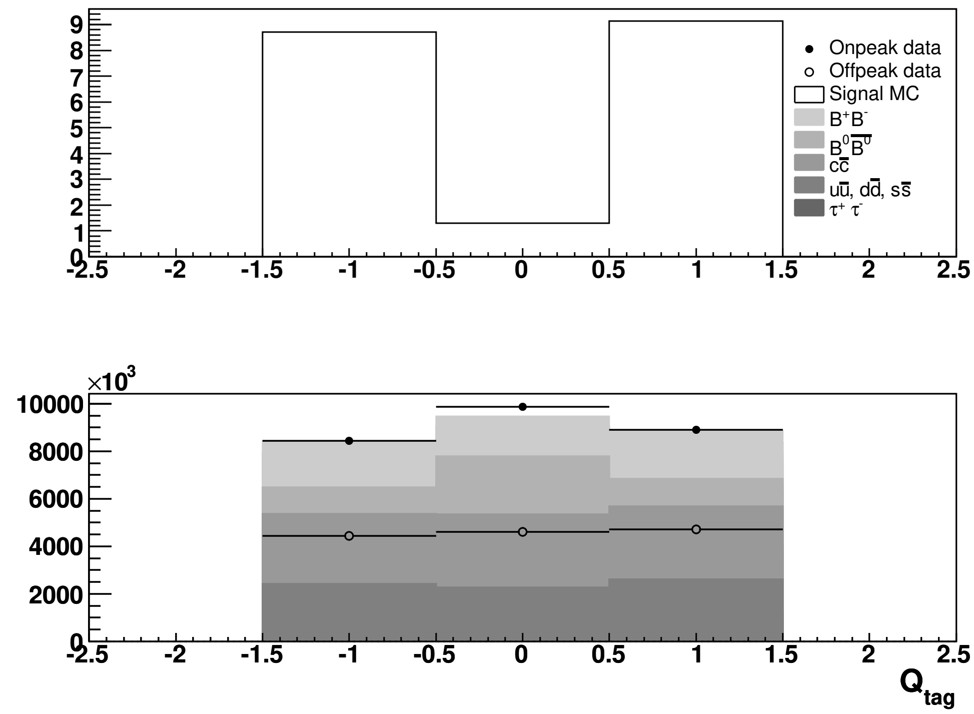

Figure 1: Q_{tag} distribution for skimmed events. Top : Signal Monte Carlo is scaled to $\mathcal{B}(B^+ \to K^+\nu\overline{\nu}) = 5.2 \times 10^{-5}$. Bottom : Offpeak data and generic Monte Carlo are scaled to onpeak data luminosity.

Table 7: Cumulative effect of tag selection requirements on data and generic MC samples. Monte Carlo samples and offpeak data have been scaled to onpeak data luminosity of $208.73\,\mathrm{fb}^{-1}$.

	Onpeak	Offpeak	B^+B^-	$B^0\overline{B}^0$	$c\overline{c}$	uds	$\tau^+\tau^-$
All Events	1 888 340 k	2 760 090 k	109 578 k	109 584 k	271 350 k	436 248 k	198 207 k
Skimmed	46 416 k	26 258 k	46 806 k	37 145 k	24 633 k	20 535 k	5 698
Q_{tag} cut	17323800	9136390	4006910	2338630	6183310	5051780	650.9
m_{ES} cut	2934220	1626900	1079570	330013	866685	724166	105.3
$\cos\theta_T$ cut	1587590	541636	863875	250032	293644	262044	38.5
$\pm$ (stat)	$\pm$ 1260	$\pm$ 742	$\pm$ 402	$\pm$ 225	$\pm$ 432	$\pm$ 410	$\pm$ 4.5

3.5 Tag Yield Correction

The excess of generic B^+B^- events in the m_{ES} signal box results in an overestimation of the reconstruction efficiency in simulated events. In order to correct that extra yield, the peaking component of the generic B^+B^- sample, or the *peaking background*, must be scaled down. We make the assumption that all the continuum and combinatoric backgrounds in the m_{ES} distribution (Fig.

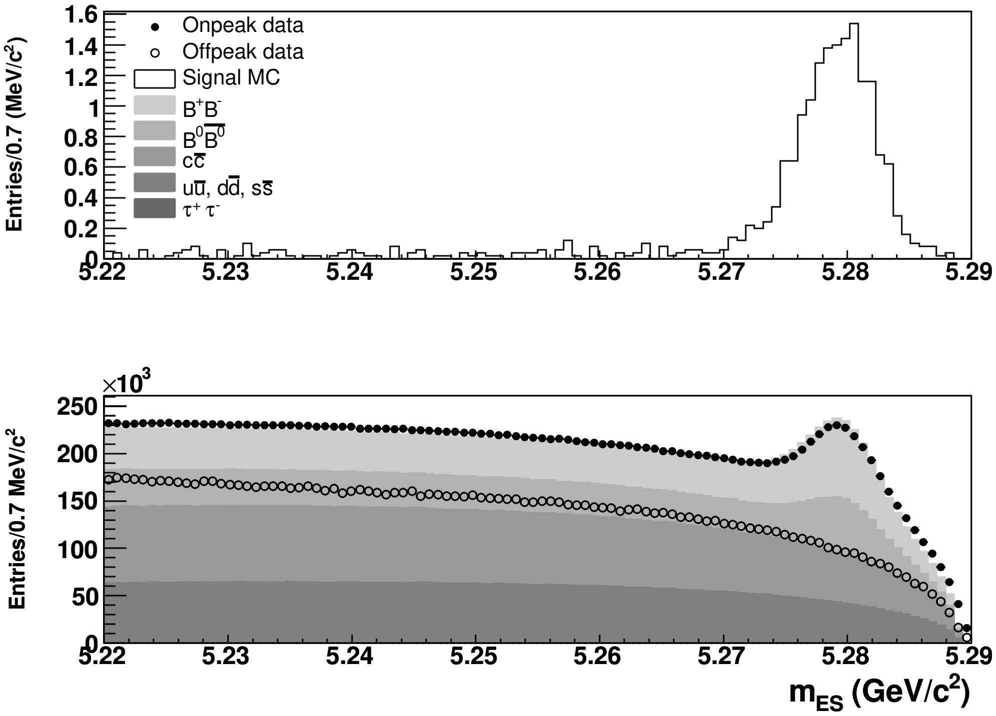

Figure 2: m_{ES} distribution for skimmed events. No other requirements are imposed. Top : Signal Monte Carlo is scaled to $\mathcal{B}(B^+ \to K^+\nu\overline{\nu}) = 5.2 \times 10^{-5}$. Bottom : Offpeak data and generic Monte Carlo are scaled to onpeak data luminosity.

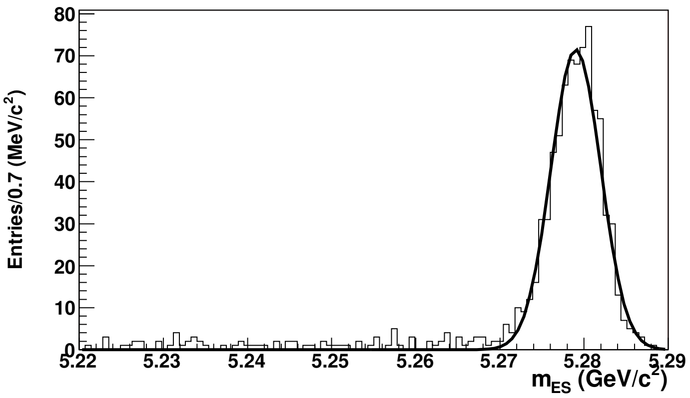

Figure 3: m_{ES} distribution for events with one charged B meson. Signal Monte Carlo is scaled to $\mathcal{B}(B^+ \to K^+\nu\overline{\nu}) = 5.2 \times 10^{-5}$.

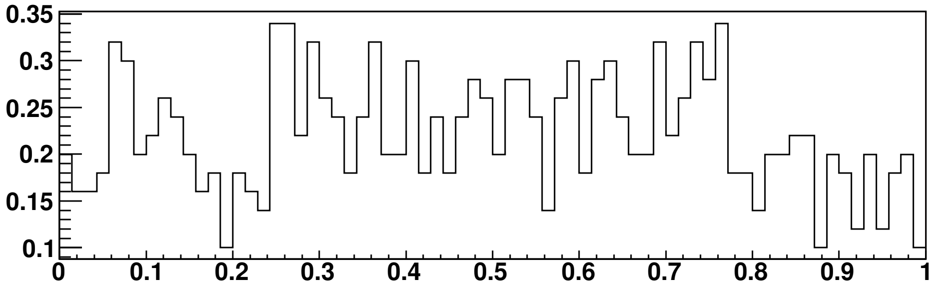

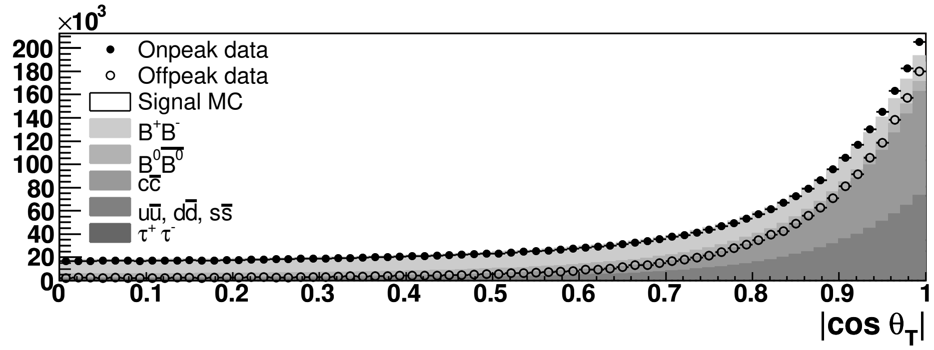

Figure 4: $|\cos\theta_T|$ distribution for events with one charged B meson, inside the m_{ES} signal box. Top : Signal Monte Carlo is scaled to $\mathcal{B}(B^+ \to K^+\nu\overline{\nu}) = 5.2 \times 10^{-5}$. Bottom : Offpeak data and generic Monte Carlo are scaled to onpeak data luminosity.

5) can be modelled by Argus functions, on the top of which lies the peak. Since there is a good agreement in the m_{ES} sideband, we conclude that the same Argus should model real and simulated events. On the other side, we want to make no assumption about the exact shape of the peak, to avoid the related systematic uncertainty.

The strategy is to fit the distribution with an Argus + Gaussian, to substract that Argus from both onpeak data and generic MC samples, and to count directly the number of events in the signal box. We do not integrate the Gaussian, so although the fit is unperfect, it behaves the same both in data an MC distributions (see Fig. 8).

We tried 8 different Argus shapes, 5 obtained by fitting an Argus on offpeak data, $c\overline{c}$, uds, continuum and $B^0\overline{B}^0$, and 3 more by fitting $B\overline{B}$, onpeak and (onpeak - offpeak) with Argus + Gaussian. The absolute peaking yields vary by about 200 events/ fb^{-1} with these shapes, but as expected, the relative yields between onpeak data and generic MC samples are stable. We get on average 2599.9 events in data and 2841.0 in MC events, which result in a scaling factor of (91.5 ± 0.8) % , where the quoted uncertainty is the worst distance from the mean (see Table 8 and Fig. 9). The m_{ES} distribution is shown in Figure 10 after the correction has been applied.

We also compute the ratio between the area of the sideband and that of the signal box, R^{areas}, for 4 of these Argus shapes. The Argus from the $B^0\overline{B}^0$ sample contains more events in the peaking region due to "pseudo-peaking" events, surely present in data, so it weights a lot in the average. We assign a value of 0.29 ± 0.04 (syst) and a systematic uncertainty of 4% to include the other

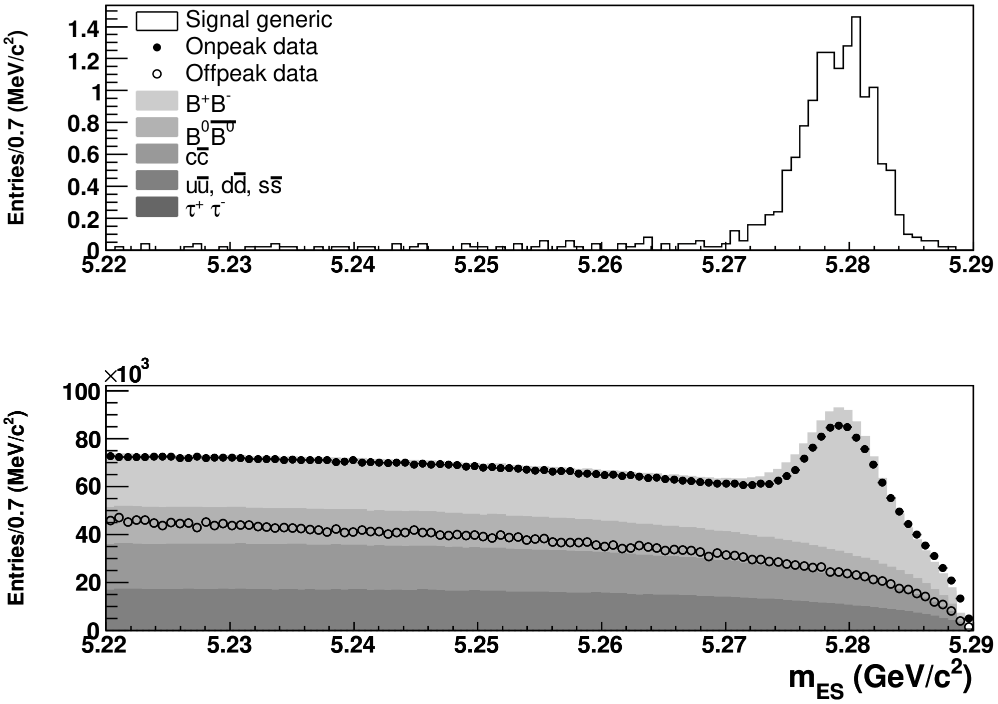

Figure 5: m_{ES} distribution for events with one charged B meson and $|\cos\theta_T| < 0.85$. Top : Signal Monte Carlo is scaled to $\mathcal{B}(B^+ \to K^+\nu\overline{\nu}) = 5.2 \times 10^{-5}$. Bottom : Offpeak data and generic Monte Carlo are scaled to onpeak data luminosity.

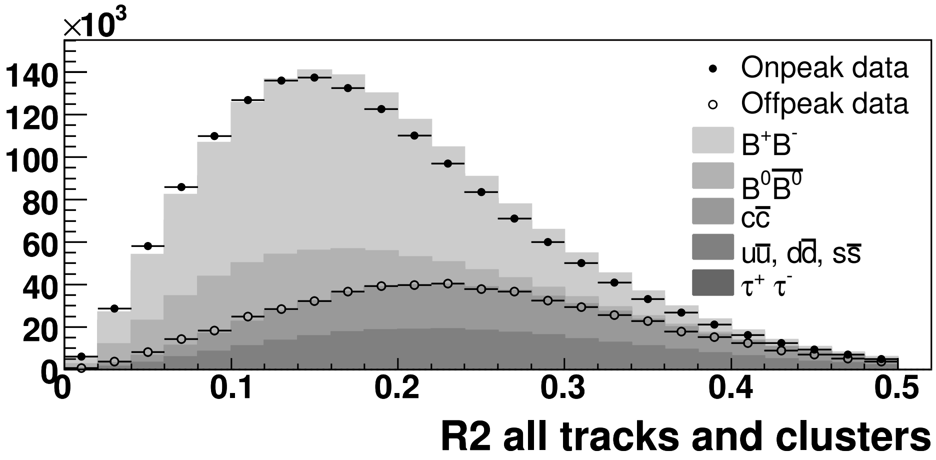

Figure 6: R2 of all tracks and clusters, for events with one charged B meson, inside the m_{ES} signal box, and with $|\cos\theta_T| < 0.85$. Offpeak data and generic Monte Carlo are scaled to onpeak data luminosity.

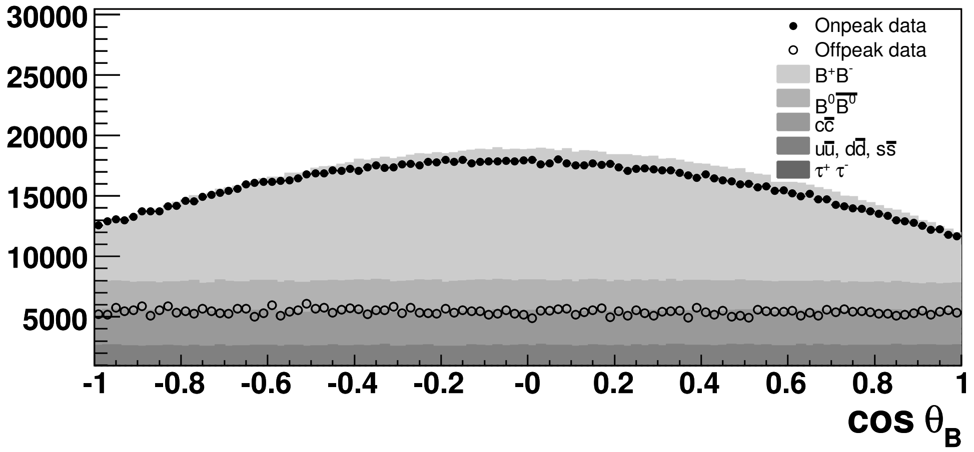

Figure 7: $\cos\theta_B$ distribution for events with one charged B meson, inside the $m_{\rm ES}$ signal box, and with $|\cos\theta_T| < 0.85$. Offpeak data and generic Monte Carlo are scaled to onpeak data luminosity.

ratios in the first σ. We did not computed that ratio for samples with a peaking component, nor for the $\tau^+\tau^-$ generic MC sample due to low statistics.

Table 8: Comparison of peaking yield for onpeak data and scaled generic MC samples, and ratio of sideband/signal-box areas, for different Argus shapes.

Argus from :	*uds*	$c\overline{c}$	continuum	offpeak	$B^0\overline{B}^0$	$B\overline{B}$	On-Off	Onpeak
OnPeak Yield	2643.0	2648.0	2653.5	2687.1	2562.6	2580.8	2478.1	2546.4
Generic MC Yield	2874.4	2880.2	2884.3	2932.8	2802.3	2822.7	2733.6	2797.7
Ratio of Yields	91.9%	91.9%	92.0%	91.6%	91.4%	91.4%	90.7%	91.0%
Ratio of Areas	27.7%	27.6%	–	25.8%	29.8%	–	–	–

3.6 Tag B Reconstruction Efficiency

The tagging efficiency $\varepsilon_{\rm tag}$ is the ratio between the number of B_{tag} and the number of events produced in signal MC. In order to increase the accuracy and precision on $\varepsilon_{\rm tag}$, we use three samples of signal MC events with similar topology, $B^+ \to K^+\nu\overline{\nu}$, $B^+ \to K^{*+}\nu\overline{\nu}$ and $B^+ \to \pi^+\nu\overline{\nu}$. We apply consecutively the requirements on $Q_{\rm tag}$, on $m_{\rm ES}$ and on $\cos\theta_T$ on each sample and observe that $\varepsilon_{\rm tag}$ agrees within error : we conclude that the reconstruction efficiency is common for all modes with that topology. The three samples can thus be combined and we obtain a value of $(0.244 \pm 0.006 \text{ (stat)})$ % (see Table 9).

Since these MC signal events are part of the peaking component in $m_{\rm ES}$, we believe that their reconstruction efficiencies have been overestimated, so $\varepsilon_{\rm tag}$ must be scaled down by the correction factor. The tagging efficiency, after the yield correction is applied, is found to be

$$\varepsilon_{\rm tag} = (0.244 \pm 0.006 \text{ (stat)})\ \% \times 91.5\ \% \ = (0.224 \pm 0.009 \text{ (stat) })\ \%$$

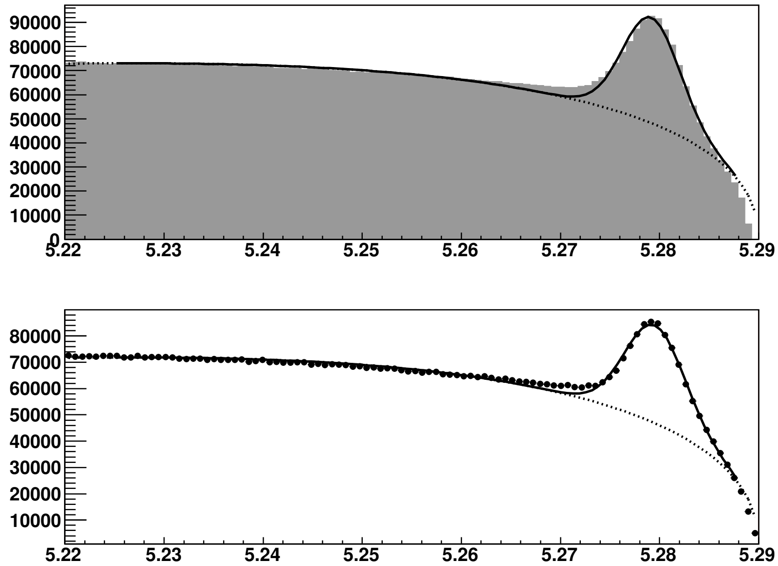

Figure 8: m_{ES} distributions for events with $Q_{\mathrm{tag}} = \pm 1$ and $|\cos\theta_T| < 0.85$. Thick points are onpeak data, dark grey is generic MC sample, thick line is an Argus + Gaussian fit, and thin line is the fitted Argus function alone. In this plot, the Argus shape parameters were found by fitting tagged $B^0\overline{B}^0$ events.

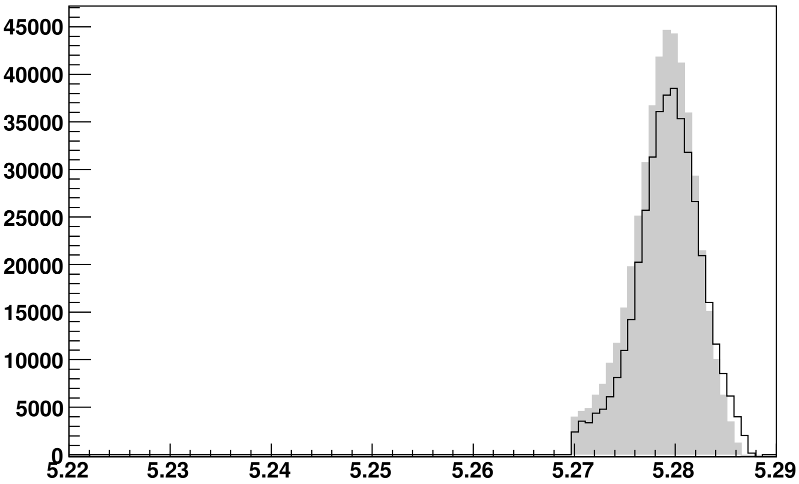

Figure 9: Peaking background in onpeak data (line) and generic MC sample (grey), after substracting an Argus function with shape parameters found by fitting tagged $B^0\overline{B}^0$ events.

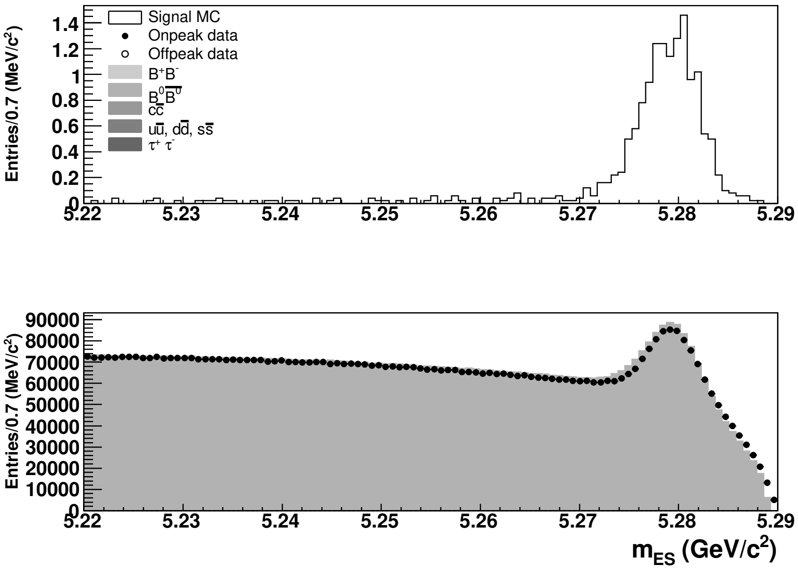

Figure 10: m_{ES} distribution for events with one charged B meson and $|\cos\theta_T| < 0.85$, after the correction on the peak yield has been applied. Top : Signal Monte Carlo is scaled to $\mathcal{B}(B^+ \to K^+\nu\overline{\nu}) = 5.2 \times 10^{-5}$. Bottom : Offpeak data and generic Monte Carlo are scaled to onpeak data luminosity.

Table 9: Cumulative effect of tag selection requirements on signal MC. Monte Carlo has been scaled to onpeak data luminosity.

	$B^+ \to K^+\nu\overline{\nu}$	$B^+ \to K^{*+}\nu\overline{\nu}$	$B^+ \to \pi^+\nu\overline{\nu}$	Combined
Produced	5 698.36	28 492	10 958	
Skimmed	23.31	175	47.9	
$Q_{\mathrm{tag}} = \pm 1$	17.85	72.55	37.30	
m_{ES} signal box	15.48	54.47	32.68	
$\lvert\cos\theta_T\rvert < 0.85$	13.70± 0.52	47.29± 1.90	29.22± 2.31	
$\varepsilon_{\mathrm{tag}}$ (± stat)	$(0.240 \pm 0.009)\%$	$(0.244 \pm 0.010)\%$	$(0.267 \pm 0.022)\%$	(0.244 ± 0.006) %

4 B_{sig} Selection

In this section, we describe the selection requirements applied on the signal side of the event. In subsection 4.1 and 4.3, we compare the current and previous analysis strategies and the blind analysis technique. Subsections 4.4 and 4.6 focus on the signal side tracks and clusters respectively and motivates the selection requirements that optimize the sensitivity to our signal. In all the plots that are presented, the correction on the yield of the peaking component has not been applied.

The momentum of the recoiling B_{sig} is assumed to be exactly opposite to that of the B_{tag}, and is used to boost various quantities in the B_{sig} rest frame. We denote X^B a quantity X computed in that frame, and X^* a quantity boosted to the CM frame.

4.1 Analysis strategy

4.1.1 Previous analysis

The previous BABAR analysis selected tagged events with only one signal side track whose charge was opposite to Q_{tag}. The track had to be idendified as a tight kaon and had to lie within the DIRC acceptance. Events with tight π^0 candidates, with total cluster energy above 250 MeV, or with more than 7 clusters (on the signal side), were suppressed, as well as events whose missing momentum vector points in the beam pipe [17].

It was thus rejecting "dirty" signal events with a few extra soft tracks on the signal side, or with $N_{\text{extra}} > 0$, regardless of their origin or features. For example, an event containing the $B^+ \to K^+\nu\overline{\nu}$ process on the signal side and with two soft tracks coming from photon conversion would be discarded, even though the process really occured.

4.1.2 Current Analysis

The current analysis has a dataset 2.5 times bigger and includes some of the dirty events. We select the kaon with the highest momentum, and then explore the nature of the additional tracks and clusters. Some of the selection criteria are taken from the previous analysis and re-optimized, and some new restrictions are added.

The algorithm is verified by looking at the "true" nature of the selected kaons (*truth-matching*) on the signal Monte Carlo sample : they are all coming from the $B^+ \to K^+\nu\overline{\nu}$ process. In one event, the true signal K^+ decayed into a π^+ within the detector ; the track was identified as a kaon, truth-matched to a pion, which was the daughter of the signal K. Such an event is to be accepted, hence the algorithm's efficiency is 100% in signal MC.

4.2 Optimization Strategy

In this analysis, we apply first a set of rather non-restrictive criteria, or "loose" criteria, that preserve most of our signal events (S). We then reject a lot of background events (B) by constraining the topology (i.e. one hard kaon, a few extra tracks...). We fine tune the signal to background sensitivity with only two variables : the kaon momentum and the left over energy in the signal side of the event. In this last step, we pick a selection for one of the two variable and, by varying the value of the selection of the other variable, we maximize the sensitivity, defined here as

$$sensitivity = \frac{\mathrm{S}}{\sqrt{\mathrm{S}+\mathrm{B}}} \tag{5}$$

We tried different combinations and kept the global maximum.

4.3 Blinding Strategy

After applying consecutively a few B_{sig} selection criteria, the statistics of the onpeak data start to go low, and the signal could potentially become dominant in specific regions of some plots. It would thus be easy to play with a set of selection requirements on a event-by-event basis, and the final result would thus be biased. In order to avoid this sort of situation, we do not look at the onpeak data unless there is at least 10 times as much generic MC background events as potential MC signal in any bin of any plot. This potential signal is represented by a dashed line in some histograms.

4.4 Tracks

Tracks in the `chargedTracks` list have non-zero charges and are assigned the pion mass by default. The number of signal side tracks per event, N_{trk}, is plotted in Figure 11 for events with a B_{tag}. MC events have on average fewer tracks per event than data (7.25 in MC compared to 7.58 in data). To reduce the size of the ntuple, a loose selection is applied and rejects events with $N_{\mathrm{trk}} > 7$. The momentum spectrum of the tracks, p^B_{trk}, shows a good agreement above 1 GeV/c, as shown in Figure 12, but data contain more tracks with momentum between 0.15 and 0.85 GeV/c. The pile up of low momentum tracks in the signal MC comes from extra tracks, and disappears if we plot the distribution for hardest track on the signal side of the event (Figure 13).

It is interesting to note that this discrepancy is improved in a low multiplicity environment : Figures 14 and 15 show again the momentum spectrum of the tracks and of the hardest track only, but for events with $N_{\mathrm{trk}} < 4$.

4.5 Candidate Kaon, Extra Tracks

In this analysis, we select the hardest track on the signal side, and require afterwards that it is a tight kaon with a charge opposite to Q_{tag}. In a $B^+ \to K^+\nu\overline{\nu}$ event, a kaon going in the beam pipe would leave no trace, and since the neutrino system is undetected, the event would look like $B \to$ *invisible*. Moreover, the detector will not be efficient at differentiating pions from kaons if the track does not enter in the Detector of Internally Reflected Cherenkov light (DIRC). To avoid these situations, $K^{\pm}$ candidate must fall in the angular acceptance of the DIRC, defined as $|\cos\theta^*_{trk}| < 0.85$, where $\cos\theta^*_{trk}$ is the angle between the tracks trajectory and the beam pipe, calculated in the CM frame (see Figure 16). We observe a discrepancy near $\cos\theta^*_{trk} = 1$: there is an unmodelled “bump” in B^+B^- MC samples.

In a signal event, the other signal side tracks do not come from the decay of the B_{sig}. They are $K^{\pm}$, $\pi^{\pm}$, $\mu^{\pm}$ or $e^{\pm}$, coming from a mis-reconstruction of the B_{tag} during the skimming process, or from photon conversion. Figure 17 presents the number of extra tracks for tagged events with a good kaon candidate. In this analysis, we incorporate some “dirty” events with up to 2 extra tracks, but we reject events with $N_{\mathrm{extra}} < 3$, in which the selected B meson is most likely a combinatoric background. This choice of selection gets rid of the poor MC-data agreement observed in $N_{\mathrm{extra}} > 3$.

The electric charge of the extra tracks Q_{extra} is shown in Figure 18, and generic MC samples is in a good agreement with data.

The $p^*_{\rm trk}$ distribution and the total energy of the extra tracks is shown in Figures 19 and 20 for events with a kaon candidate and $N_{\rm extra} < 3$. There is a small discrepancy for events with track momentum smaller than 0.7 GeV/c, and with total track energy smaller than 0.8 GeV. Data (MC) have on average 7.58 (7.25) extra tracks, with a momentum of 329 (306) MeV/c.

We always plot the momentum of the kaon candidate in the B_{sig} frame, since it is compared to a theoretical model in which the spectrum of $B^+ \to K^+\nu\overline{\nu}$ events are calculated in the rest frame of the decaying B mesons. Figure 21 plots the momentum distribution of the kaon for events satisfying the requirement on $N_{\rm extra}$. Cocktail and generic signal are stacked to show the distribution with higher statistics. There is an excess of generic Monte Carlo in the region 0.7-2.0 GeV/c, which will be discussed in section 9. Good kaon candidates are required to satisfy $p^B_{\rm kaon} > 1.1\,{\rm GeV}/c$ in order to maximize the sensitivity.

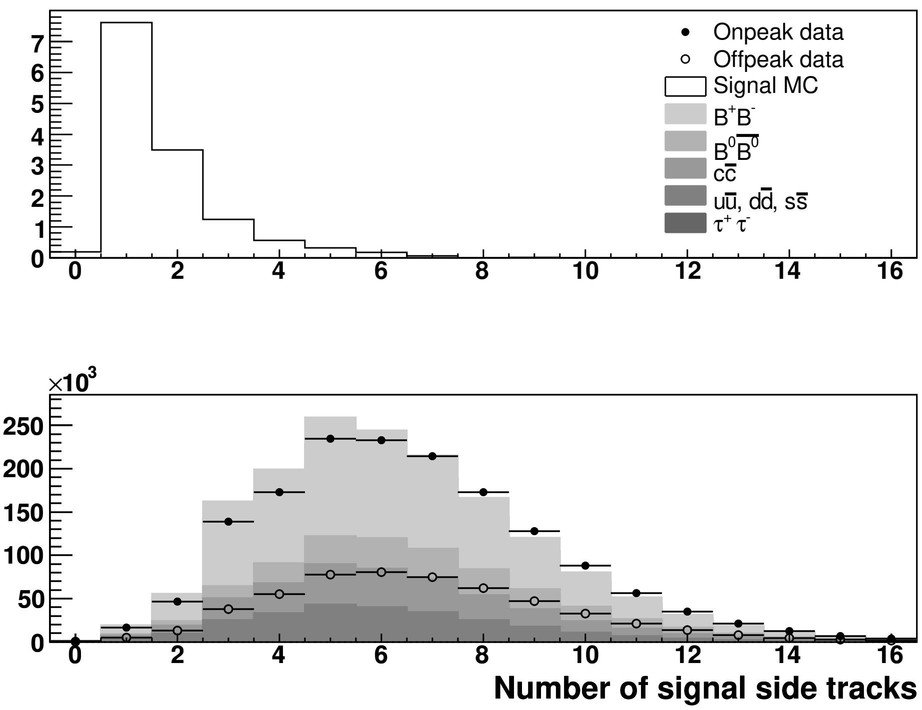

Figure 11: N_{trk} for tagged events. Top : Signal Monte Carlo is scaled to $\mathcal{B}(B^+ \to K^+\nu\overline{\nu}) = 5.2 \times 10^{-5}$. Bottom : Offpeak data and generic Monte Carlo are scaled to onpeak data luminosity.

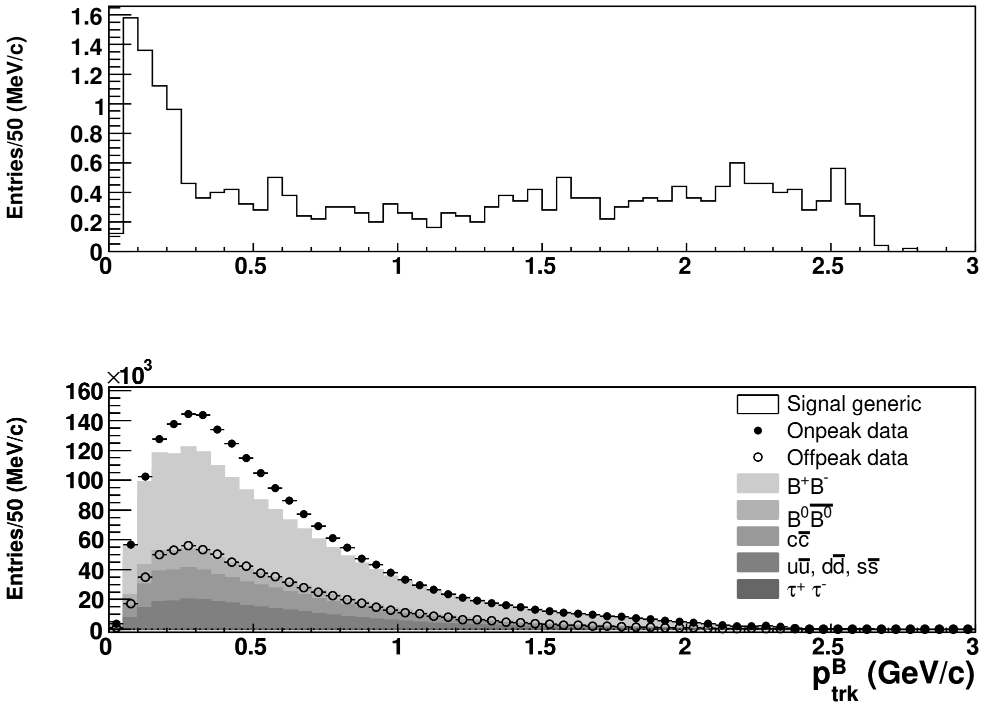

Figure 12: p_{trk}^{B} distribution for tagged events with N_{trk} <7. Top : Signal Monte Carlo is scaled to $\mathcal{B}(B^+ \to K^+\nu\overline{\nu}) = 5.2 \times 10^{-5}$. Bottom : Offpeak data and generic Monte Carlo are scaled to onpeak data luminosity.

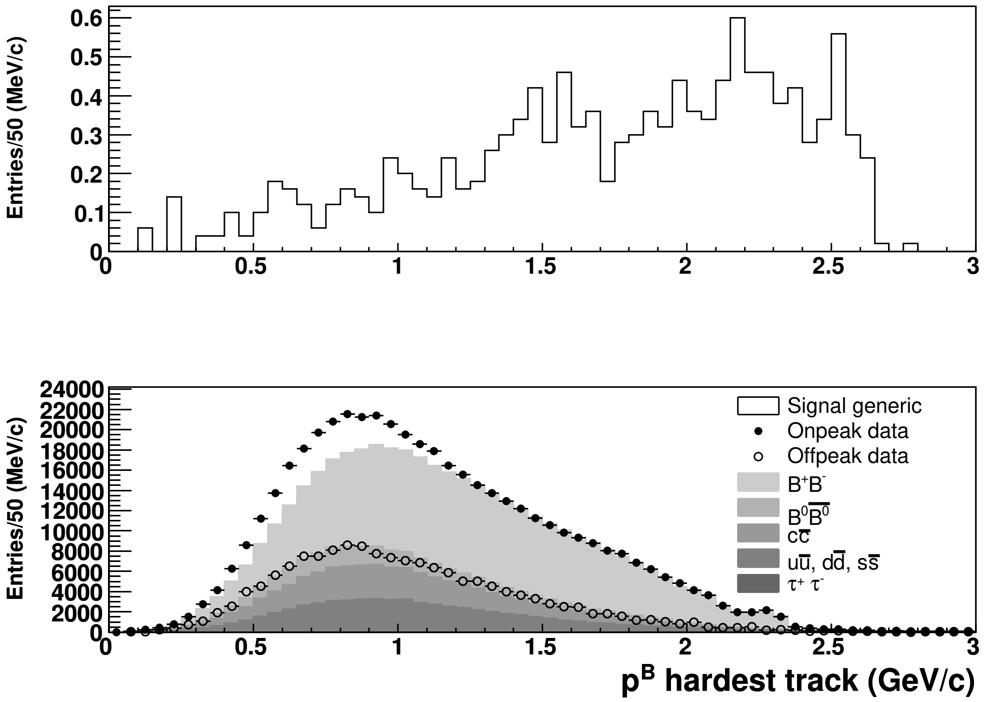

Figure 13: $p^B_{\rm trk}$ distribution for the track with the highest momentum, for tagged events with $N_{\rm trk}$ $<$7. Top : Signal Monte Carlo is scaled to $\mathcal{B}(B^+ \to K^+\nu\overline{\nu}) = 5.2 \times 10^{-5}$. Bottom : Offpeak data and generic Monte Carlo are scaled to onpeak data luminosity.

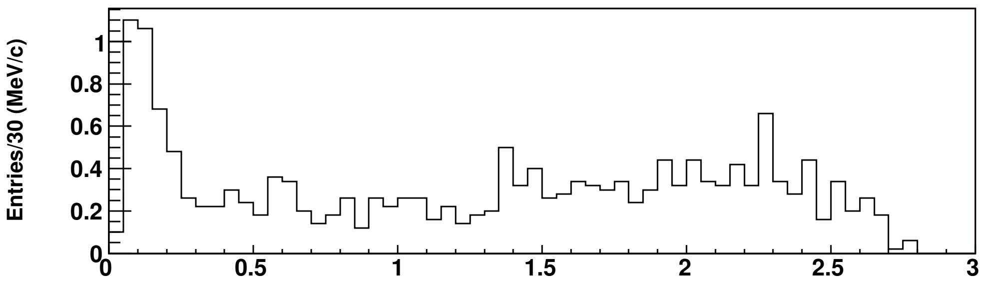

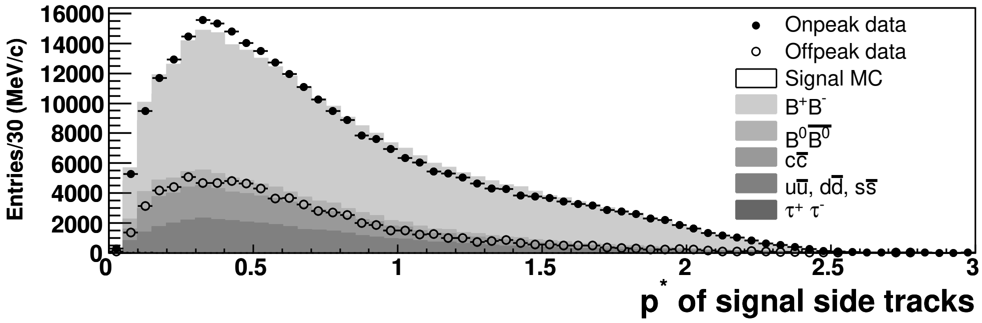

Figure 14: $p^*_{\rm trk}$ distribution for tagged events with $N_{\rm trk}$ <4. Top : Signal Monte Carlo is scaled to $\mathcal{B}(B^+ \to K^+\nu\overline{\nu}) = 5.2 \times 10^{-5}$. Bottom : Offpeak data and generic Monte Carlo are scaled to onpeak data luminosity.

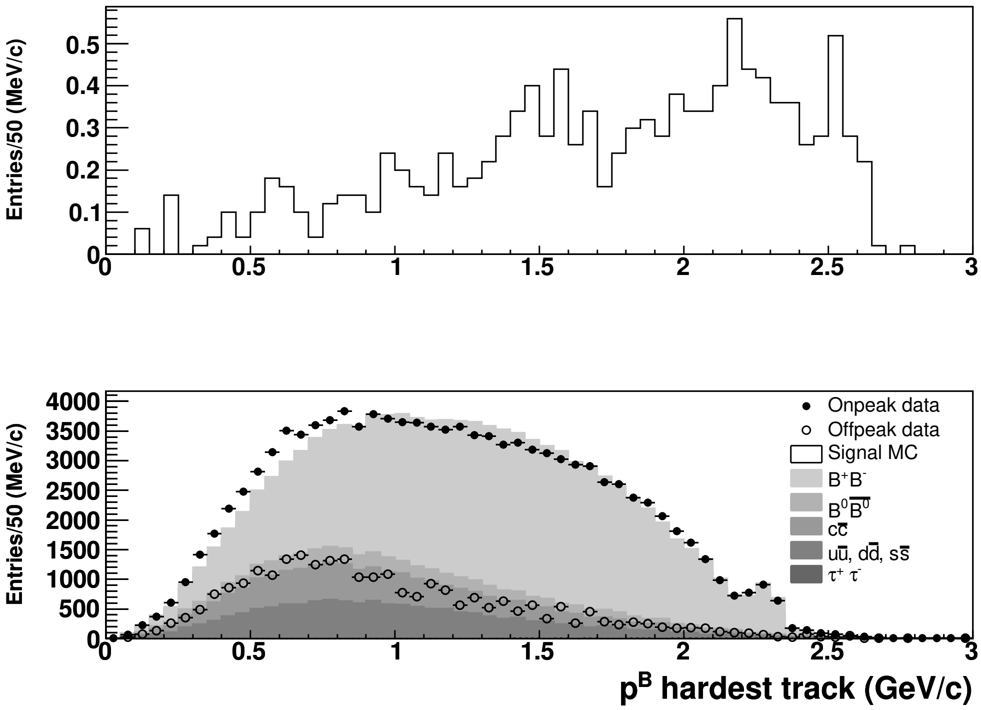

Figure 15: p^{B}_{trk} distribution for the track with the highest momentum, for tagged events with N_{trk} <4. Top : Signal Monte Carlo is scaled to $\mathcal{B}(B^{+} \rightarrow K^{+}\nu\overline{\nu}) = 5.2 \times 10^{-5}$. Bottom : Offpeak data and generic Monte Carlo are scaled to onpeak data luminosity.

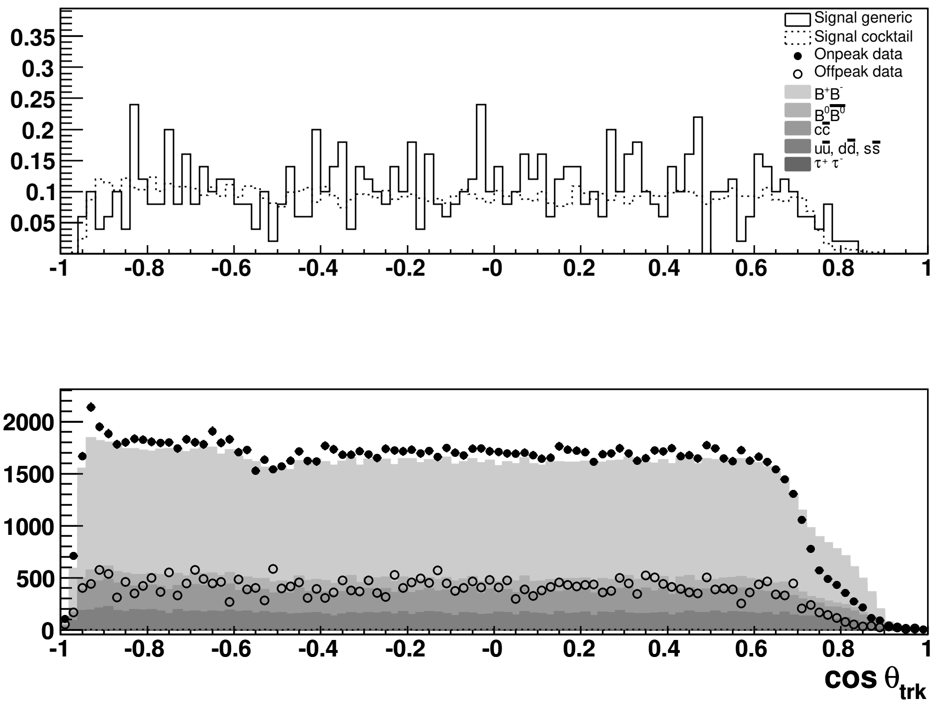

Figure 16: $\cos\theta^*_{trk}$ distribution for candidate kaons in tagged events with $N_{\rm trk}$ <7. Top : Signal Monte Carlo is scaled to $\mathcal{B}(B^+ \to K^+\nu\overline{\nu}) = 5.2\times 10^{-5}$. Bottom : Offpeak data and generic Monte Carlo are scaled to onpeak data luminosity.

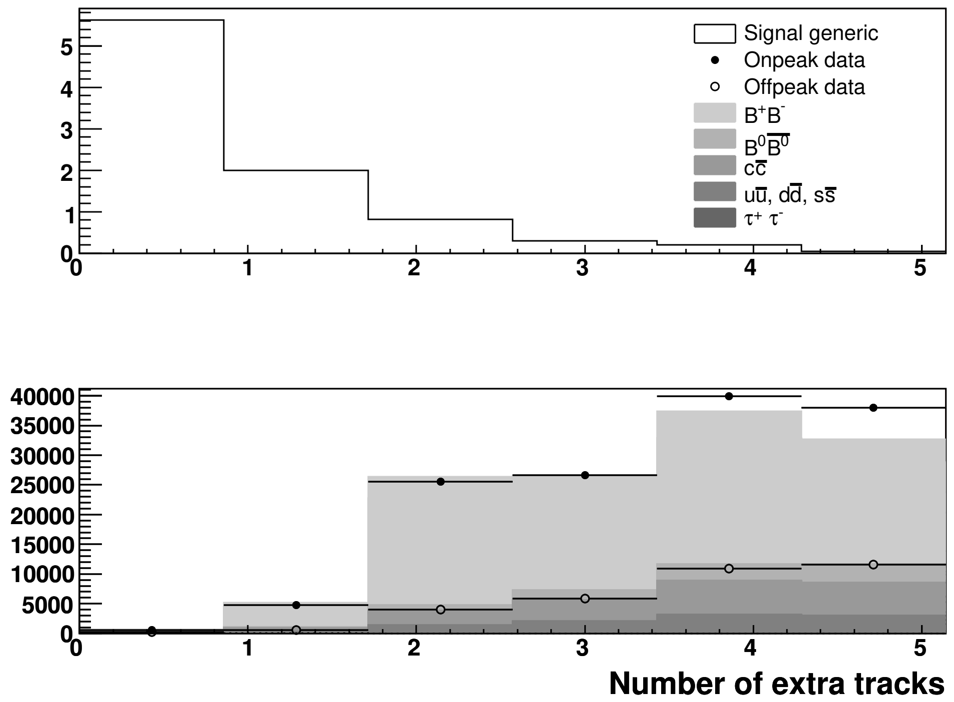

Figure 17: Number of extra tracks on signal side for tagged events with a good kaon candidate. Top : Signal Monte Carlo is scaled to $\mathcal{B}(B^+ \to K^+\nu\overline{\nu}) = 5.2 \times 10^{-5}$. Bottom : Offpeak data and generic Monte Carlo are scaled to onpeak data luminosity.

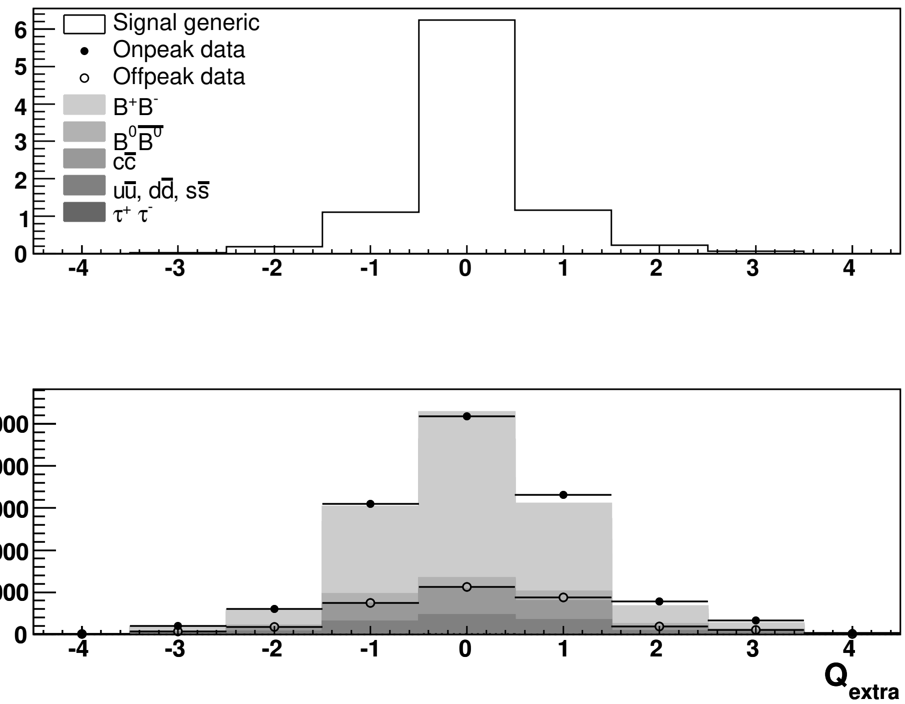

Figure 18: $Q_{\rm extra}$ for tagged events with a good kaon candidate and $N_{\rm trk}$ <7. Top : Signal Monte Carlo is scaled to $\mathcal{B}(B^+ \to K^+\nu\overline{\nu}) = 5.2 \times 10^{-5}$. Bottom : Offpeak data and generic Monte Carlo are scaled to onpeak data luminosity.

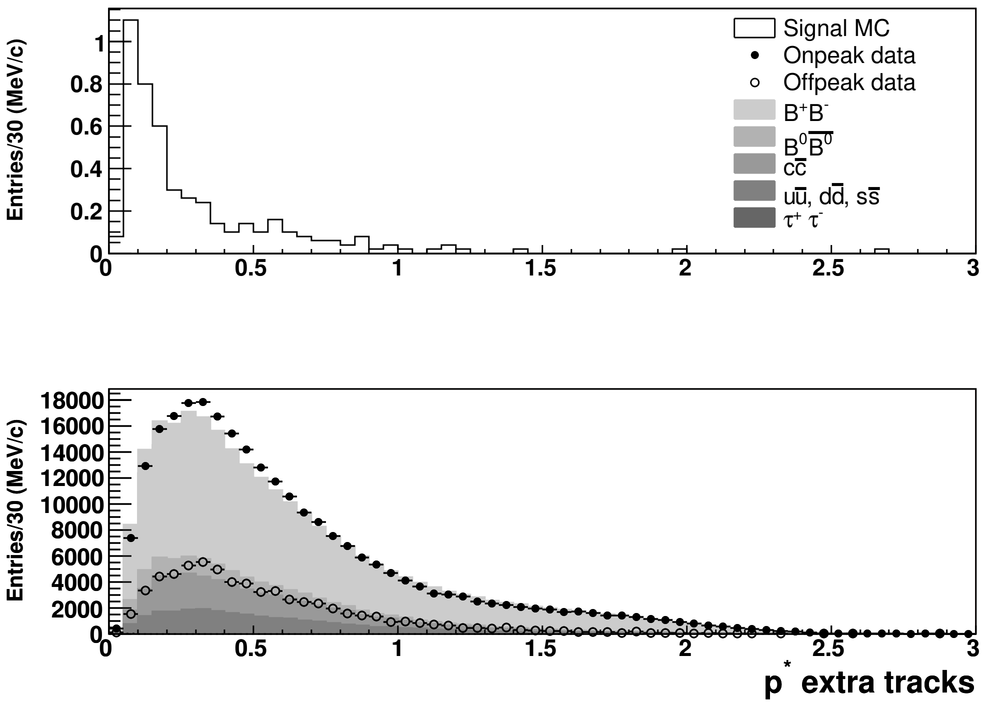

Figure 19: $p^*_{\rm extra}$ distribution, for tagged events with a good kaon candidate and $N_{\rm trk}$ <3. Top : Signal Monte Carlo is scaled to $\mathcal{B}(B^+ \to K^+\nu\overline{\nu}) = 5.2 \times 10^{-5}$. Bottom : Offpeak data and generic Monte Carlo are scaled to onpeak data luminosity.

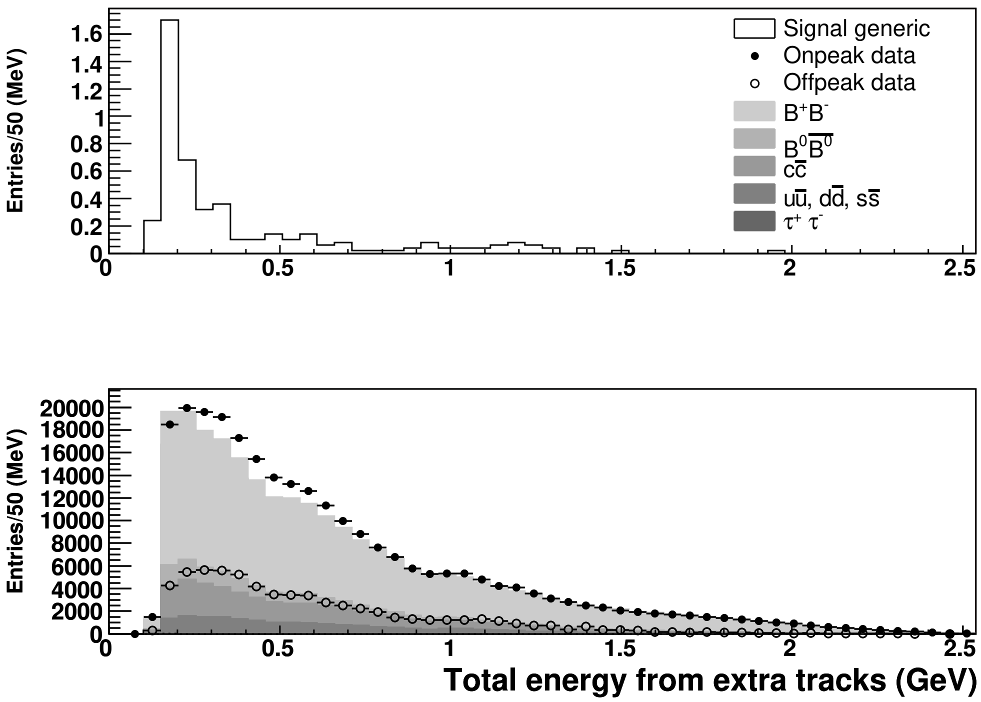

Figure 20: Total energy of extra tracks, for tagged events with a good kaon candidate and N_{trk} <3. Top : Signal Monte Carlo is scaled to $\mathcal{B}(B^+ \to K^+\nu\overline{\nu}) = 5.2 \times 10^{-5}$. Bottom : Offpeak data and generic Monte Carlo are scaled to onpeak data luminosity.

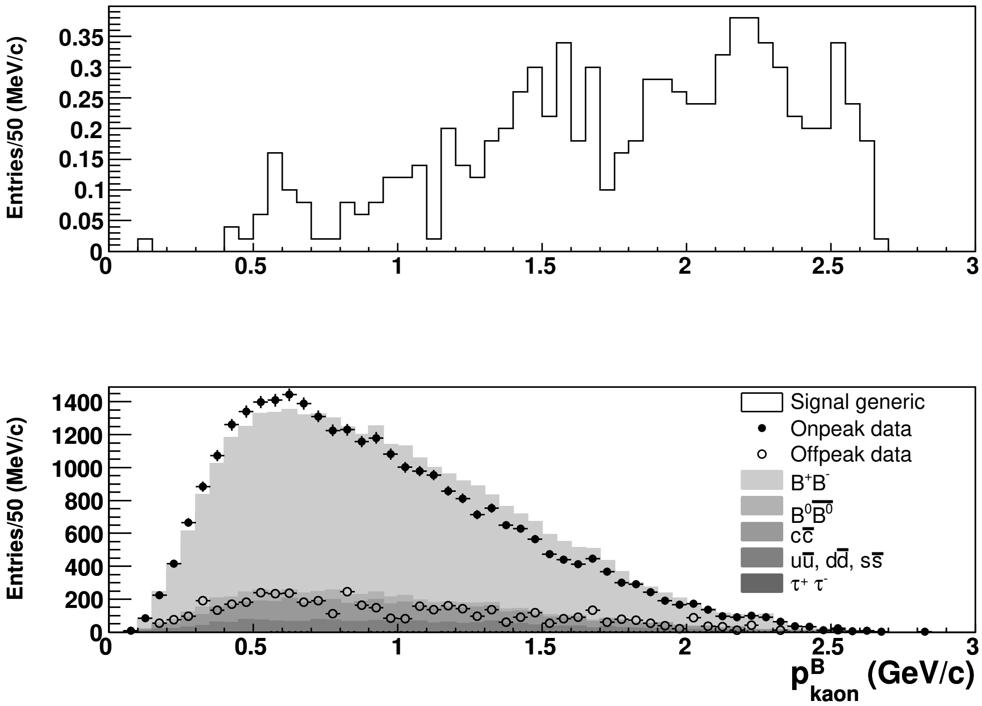

Figure 21: $p^B_{\rm trk}$ distribution of the kaon candidate for tagged events with $N_{\rm trk}$ <3. Top : Signal Monte Carlo is scaled to $\mathcal{B}(B^+ \to K^+\nu\overline{\nu}) = 5.2 \times 10^{-5}$. Bottom : Offpeak data and generic Monte Carlo are scaled to onpeak data luminosity.

4.6 Clusters

A single bump detected in the electromagnetic calorimeter (EMC) is considered as a photon unless it is matched to a charged particle in the tracking system. There is an energy threshold of 20 MeV applied on any candidate in the `calorNeutral` list. As shown in Figure 22, N_{clus}, the number of clusters for tagged events and $N_{\text{trk}} < 4$ is not in perfect agreement. It appears from the shift in the peak that data events have on average less photons per events, (11.2 in data and 12.7 in generic MC samples).

We apply a loose criteria on the multiplicity of the clusters to reject events with more than 10 clusters. Their energy spectrum, presented in Figure 23, is enlightening as it demonstrates that the multiplicity excess in MC is mainly due to photons with energy below 100 MeV. Clusters have an energy of 40 MeV in data and 28 MeV in generic MC samples. The energy spectrum of the hardest cluster per events is also shown in Figure 24 with the loose selection on N_{trk}, and it tends to be slightly more energetic in data, as seen from a shift in the peak.

4.7 π^0 Veto

A π^0 candidate is reconstructed from two signal side clusters. The mass of these candidates is shown in Figure 25 for all tagged events, without any further restrictions. Signal events are populated with these "loose" π^0 candidates, obtained by combining randomly clusters from bremsstrahlung, or photon which should have been incorporated in the B_{tag} recontruction but were not. The number of π^0 in signal events drops if we are more restrictive, so we define a "tight" candidate any π^0 whose mass is in the range $0.121 < m_{\pi^0} < 0.145$ GeV/c^2 , and we veto events with tight π^0 on the signal side. Doing so, we do not have to worry about double counting clusters in the `calorNeutral` and in the `pi0Loose` lists. Figure 26 shows the number of tight π^0 for tagged events with a $K^{\pm}$ candidate and less than three extra tracks.

4.8 Extra Energy

A typical signal event contains on average 5 photons with individual energy smaller than 200 MeV, coming from Bremsstrahlung or from the decay of the B_{tag}. Since in background events the number of clusters peaks at 10 and the energy of hard photons spreads well above 1 GeV, it is useful to look at the total neutral energy per event (Figure 27). There is a good agreement between onpeak and MC for energies of 50 to 200 MeV, and between offpeak and continuum in the whole range. The first bin shows an excess in MC events, coming from the observed discrepancy in the multiplicity of soft photons. Figure 28 shows the same distribution, but for events with less than four signal side tracks, including a kaon candidate.

At this level in the analysis, most of the background comes from the B^+B^- generic MC, and these events also have on average 1.9 tracks, appart from the kaon candidate. We can combine the energy of these extra tracks with the energy from the signal side clusters, to compute the total extra energy, E_{extra}, and improve significantly the background rejection power (see Figure 29). In a signal event, most of the extra tracks come from the tag side, so it makes sense to compute E_{extra} in the CM frame. We observe a good agreement between data and MC samples. The sensitivity is optimized when we require events to have $E_{extra} < 0.400$ GeV. We also define an E_{extra} sideband in the region $0.5 < E_{extra} < 1.5$ GeV, rich in B^+B^- events (see section 7).

Running low on statistics after applying that selection, most of the plots in the E_{extra} signal box are blind to onpeak data (see the dashed line in Figure 29).

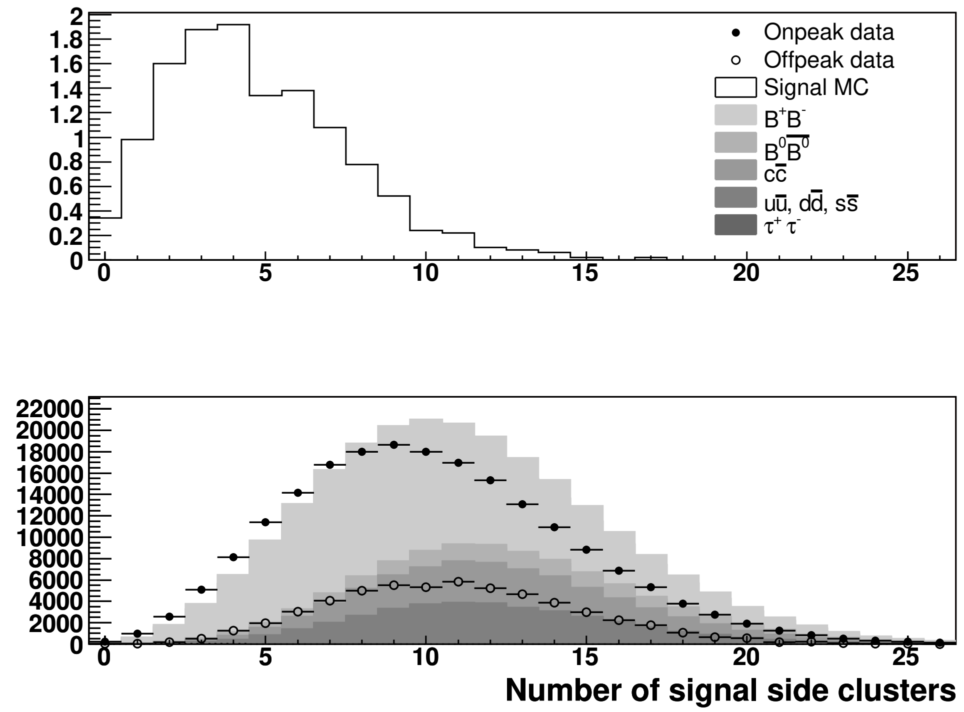

Figure 22: N_{clus} for tagged events with N_{trk} <4. Top : Signal Monte Carlo is scaled to $\mathcal{B}(B^+ \rightarrow K^+\nu\overline{\nu}) = 5.2 \times 10^{-5}$. Bottom : Offpeak data and generic Monte Carlo are scaled to onpeak data luminosity.

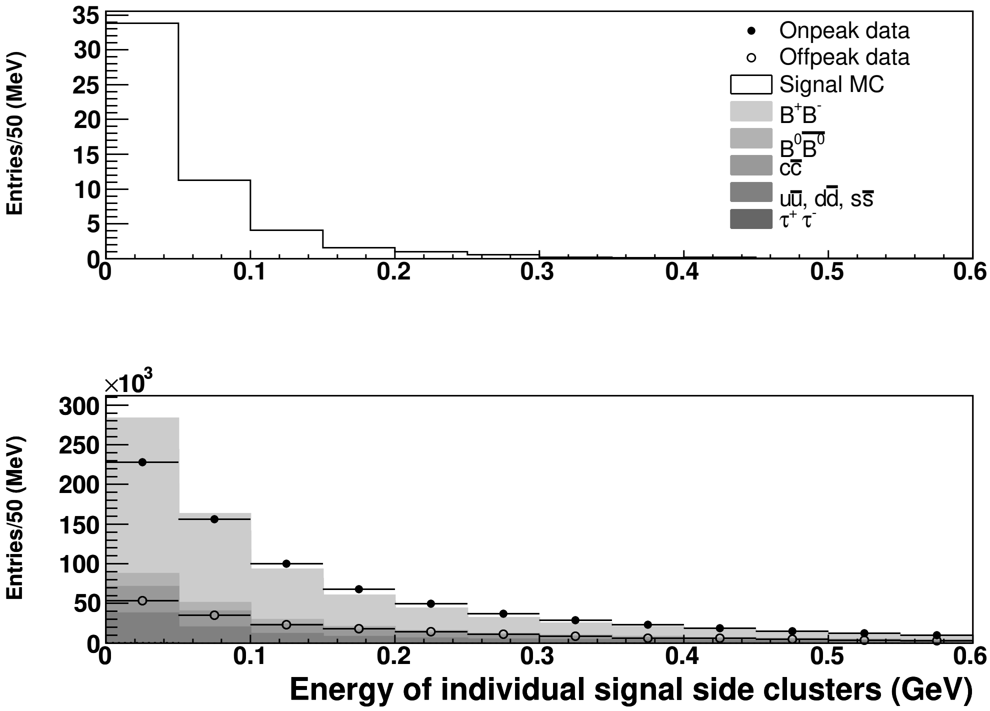

Figure 23: Energy of individual signal side clusters for tagged events with $N_{\mathrm{trk}} < 4$. Top : Signal Monte Carlo is scaled to $\mathcal{B}(B^+ \to K^+ \nu\overline{\nu}) = 5.2 \times 10^{-5}$. Bottom : Offpeak data and generic Monte Carlo are scaled to onpeak data luminosity.

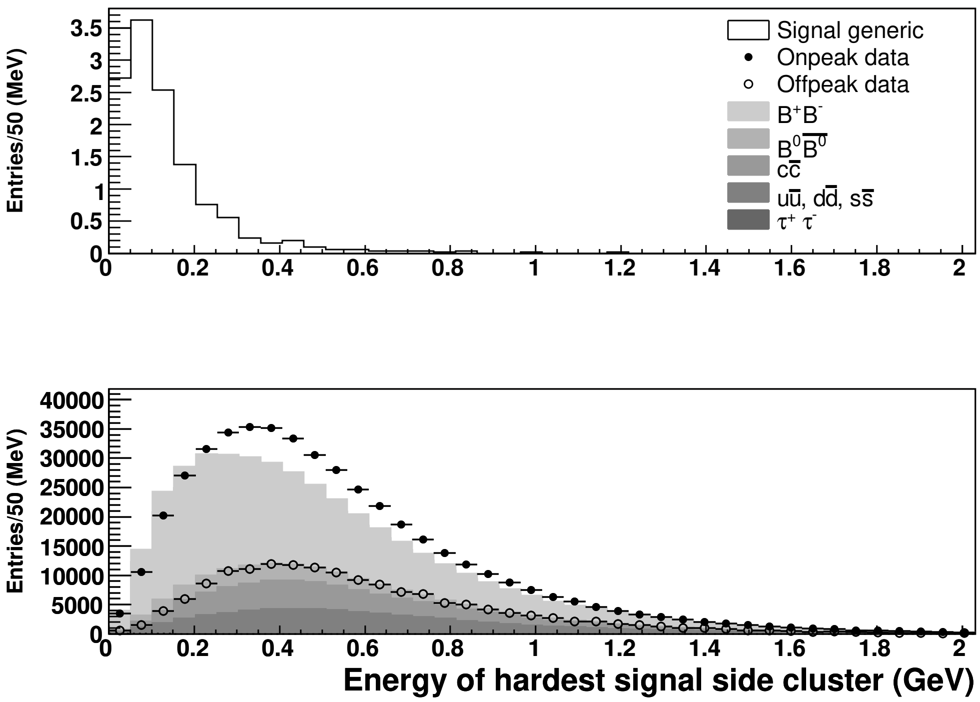

Figure 24: Energy of the hardest signal side clusters for tagged events with $N_{\mathrm{trk}} < 7$. Top : Signal Monte Carlo is scaled to $\mathcal{B}(B^+ \to K^+ \nu \overline{\nu}) = 5.2 \times 10^{-5}$. Bottom : Offpeak data and generic Monte Carlo are scaled to onpeak data luminosity.

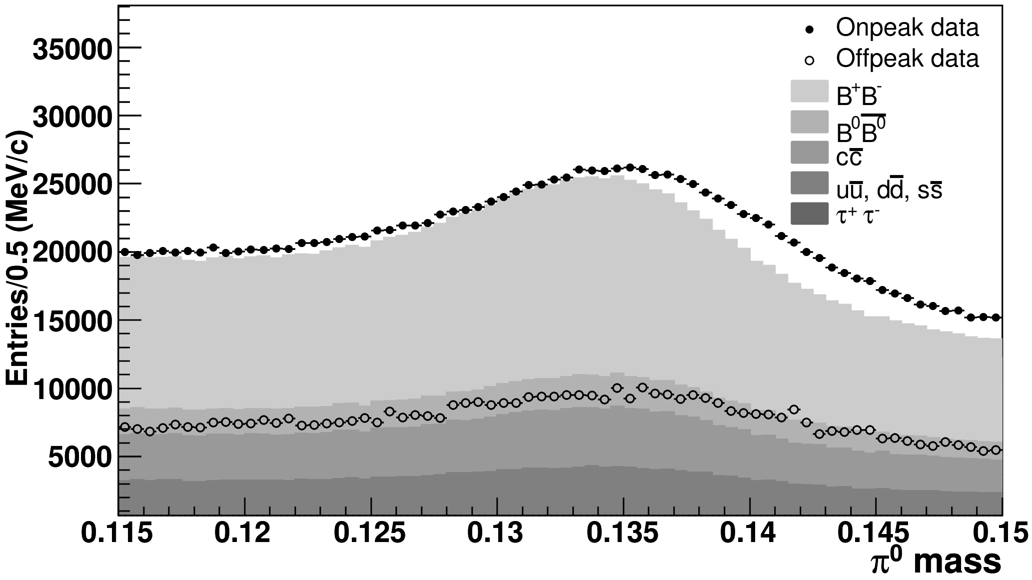

Figure 25: Mass of π^0 for tagged events. Offpeak data and generic Monte Carlo are scaled to onpeak data luminosity.

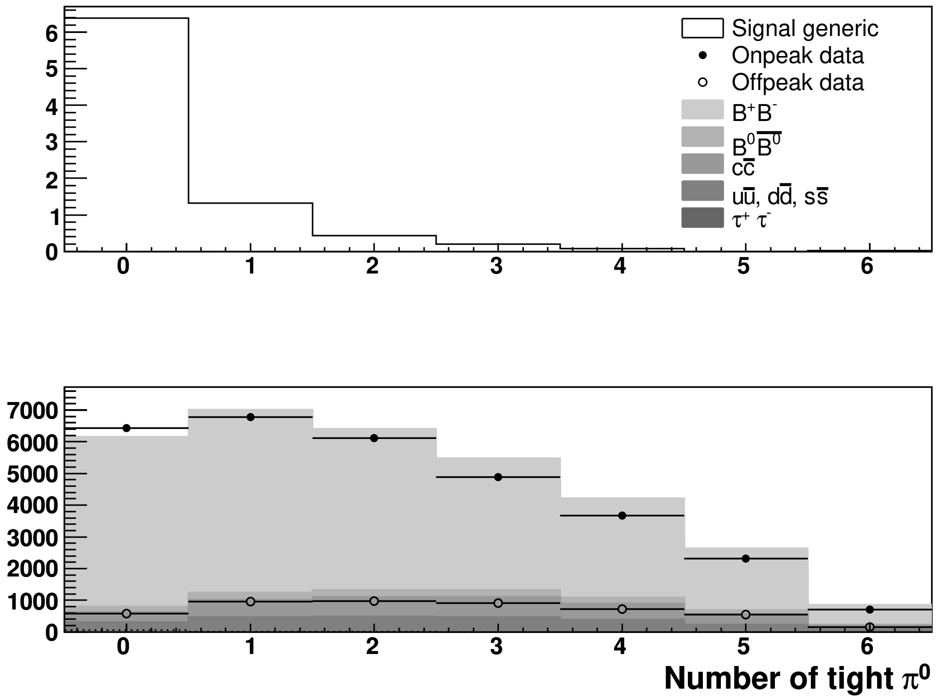

Figure 26: Number of tight π^0 candidates for tagged events with a good kaon candidate and N_{trk} <3. Top : Signal Monte Carlo is scaled to $\mathcal{B}(B^+ \to K^+\nu\overline{\nu}) = 5.2 \times 10^{-5}$. Bottom : Offpeak data and generic Monte Carlo are scaled to onpeak data luminosity.

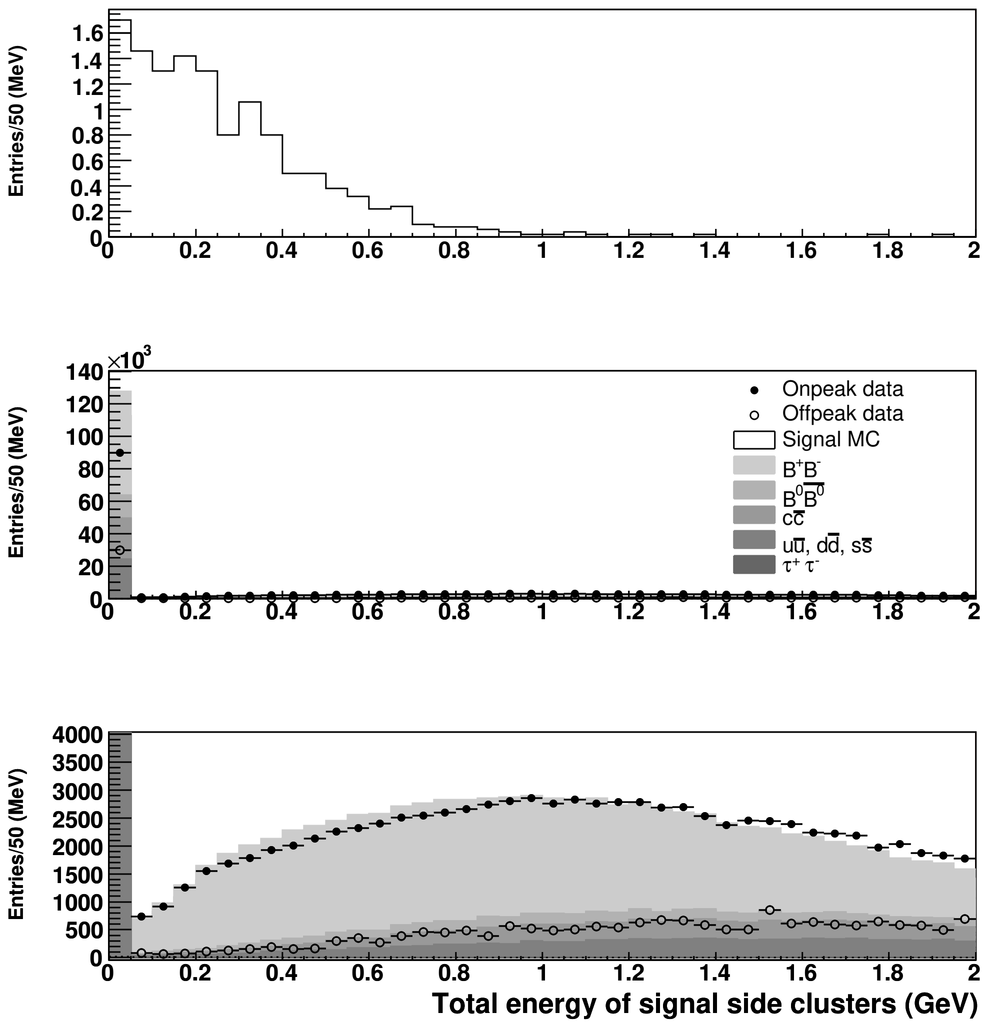

Figure 27: Total energy of signal side clusters for tagged events with $N_{\mathrm{trk}} < 4$. Top : Signal Monte Carlo is scaled to $\mathcal{B}(B^+ \to K^+\nu\overline{\nu}) = 5.2 \times 10^{-5}$. Middle and Bottom : Offpeak data and generic Monte Carlo are scaled to onpeak data luminosity.

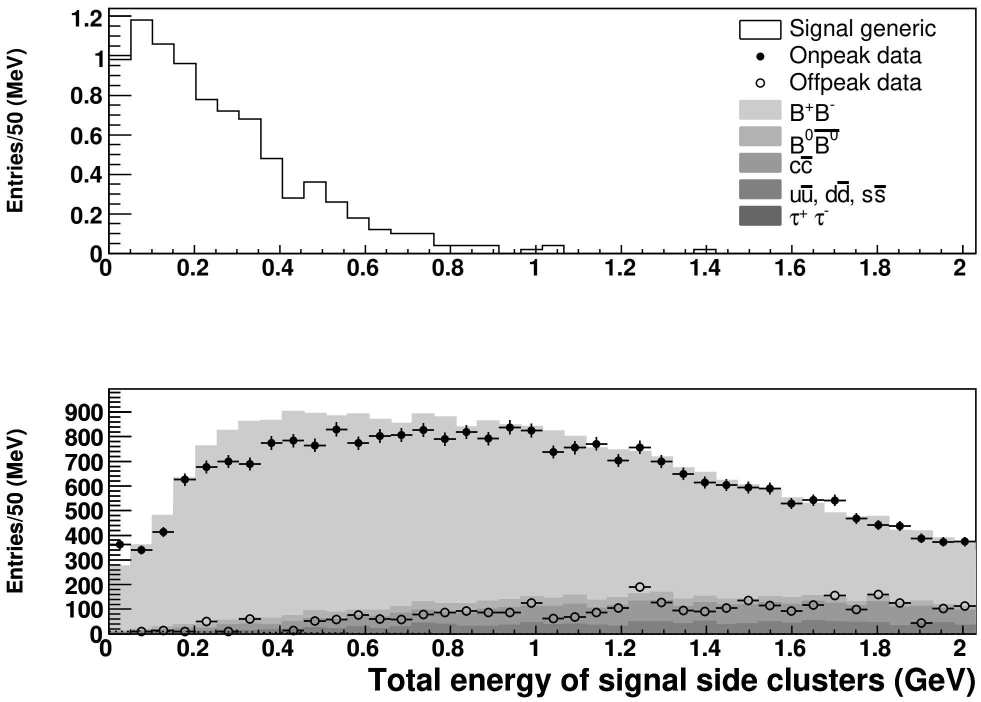

Figure 28: Total energy of signal side clusters for tagged events with a kaon candidate and $N_{\rm trk}$ <3. Top : Signal Monte Carlo is scaled to $\mathcal{B}(B^+ \to K^+\nu\overline{\nu}) = 5.2 \times 10^{-5}$. Bottom : Offpeak data and generic Monte Carlo are scaled to onpeak data luminosity.

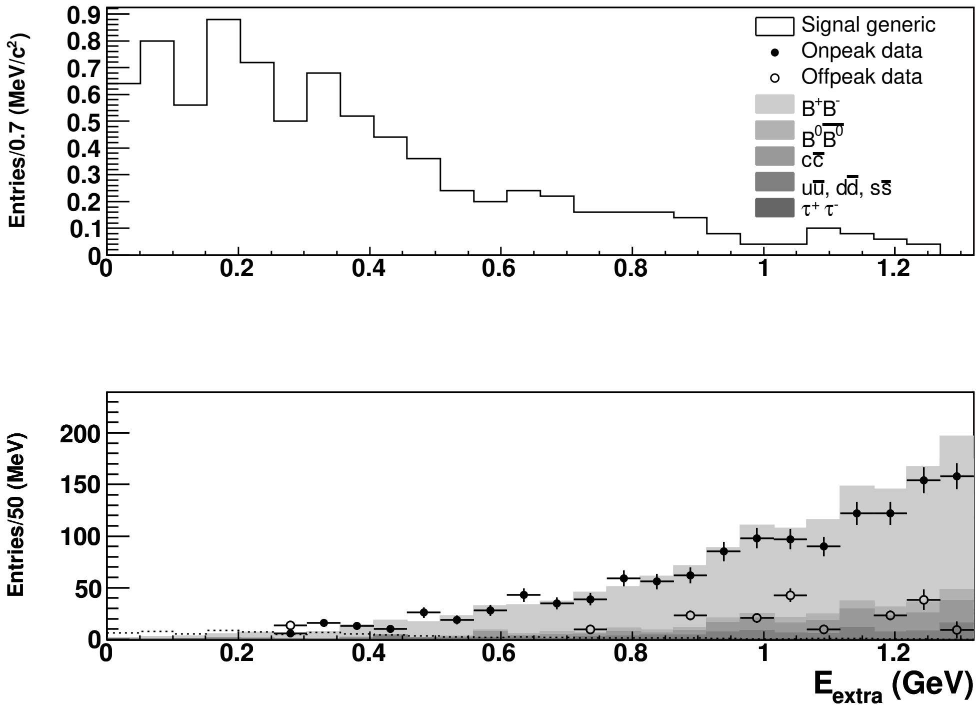

Figure 29: E_{extra} distribution for tagged events with a kaon candidate and $N_{\rm trk}$ <3. The region E_{extra} < 250 MeV is blind to onpeak data. Top : Signal Monte Carlo is scaled to $\mathcal{B}(B^+ \to K^+\nu\overline{\nu}) = 5.2 \times 10^{-5}$. Bottom : Offpeak data and generic Monte Carlo are scaled to onpeak data luminosity.

4.9 Missing Energy

In a $B^+ \to K^+ \nu\overline{\nu}$ process, the $\nu\overline{\nu}$ system is undetected, but we use the information on the missing energy to reject a last group of background events. The spectrum of the dilepton mass in a signal event could be faked by a particle leaving the detector along the beam pipe. To avoid this situation, the missing 4-vector, defined as $p^{\mu}_{miss} = p^{\mu}_{e^+beam} + p^{\mu}_{e^-beam} - p^{\mu}_{B_{tag}} - \sum p^{\mu}_{tracks} - \sum p^{\mu}_{clusters}$, is required to point away from the beam pipe. The sums are over the signal side only. Namely, we reject events that do not satisfy $-0.85 < \cos\theta_{Pmiss} < 0.90$.

This selection was cross-checked with the cocktail MC signal samples to make sure that the behavior of the signal near the end points is not a lower bound statistical fluctuation (see Figure 30). We observe that there is a small over-estimation near the region $\cos\theta_{Pmiss} = 1$ in generic MC events, but we recall that we have not corrected for the excess of peaking B^+B^- in these plots.

The B_{sig} selection criteria are summarized in Table 10.

Table 10: List of requirements on the B_{sig} candidate in the current and previous analysis.

Current analysis	Previous analysis
Kaon candidate	Kaon candidate
$\lvert\cos\theta^*_{trk}\rvert < 0.85$	$\lvert\cos\theta^*_{trk}\rvert < 0.85$
$N_{\mathrm{extra}} < 3$	$N_{\mathrm{extra}} = 0$
$E_{extra} < 0.400$ GeV	Total $E^*_{\mathrm{clus}} < 250$ MeV
$N_{\pi^0} = 0$	$N_{\pi^0} = 0$
$p^B_{\mathrm{kaon}} > 1.1\,\mathrm{GeV}/c$	$p^B_{\mathrm{kaon}} > 1.25$ GeV/c
$-0.85 < \cos\theta_{Pmiss} < 0.90$	$\lvert\cos\theta_{Pmiss}\rvert < 0.9$

4.10 $\varepsilon_{\mathrm{sig}}$

The number of events surviving the consecutive signal side cuts is presented on Table 11 for the three signal Monte Carlo samples. The signal efficiency $\varepsilon_{\mathrm{sig}}$ is defined as the number of signal events surviving the signal selection ($N^{B_{sig}}$), divided by the number of events that survived the B_{tag} selection ($N^{B_{tag}}$). $\varepsilon_{\mathrm{sig}}$ is unaffected by the tagging yield correction factor. We find

$$\varepsilon_{\mathrm{sig}} = \frac{N^{B_{sig}}}{N^{B_{tag}}} = (30.2 \pm 2.4\ (\mathrm{stat})\ )\%$$

for $B^+ \to K^+ \nu\overline{\nu}$ process.

4.11 Phase-Space Reweighting

The phase-space model used in our simulation is not believed to reproduce accurately the physics of the decay channel. The invariant mass of the dilepton system, defined as : $q^2 = (p_{e^+} + p_{e^-} - p_{B_{tag}} - p_{kaon})^2$ is shown in Figure 31 (top part) for events with a good kaon candidate.

We compare the cocktail MC events to the dynamical model [11] and we see that the latter predicts less low-q^2 events than the phase-space model, hence less high-momentum kaons. This has a direct impact on the signal efficiency, as it can potentially lower the number of signal kaons surviving the selection.

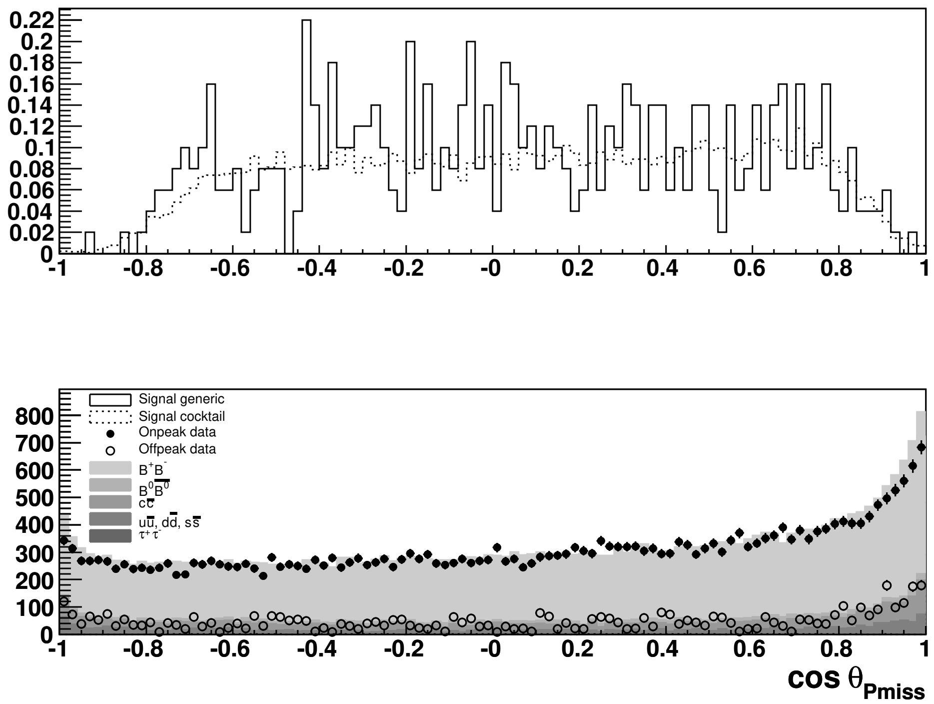

Figure 30: $\cos\theta_{Pmiss}$ for tagged events with a kaon candidate and $N_{\rm trk}$ <3. Top : Signal Monte Carlo is scaled to $\mathcal{B}(B^+ \to K^+\nu\overline{\nu}) = 5.2\times10^{-5}$. Bottom : Offpeak data and generic Monte Carlo are scaled to onpeak data luminosity.

Table 11: Effect of signal selection cuts on signal MC. Monte Carlo has been scaled to onpeak data luminosity.

	$B^+ \to K^+\nu\overline{\nu}$	$B^+ \to K^{*+}\nu\overline{\nu}$	$B^+ \to \pi^+\nu\overline{\nu}$
B_{tag}	13.70	47.29	29.22
Kaon candidate	9.36	10.65	0.58
$\lvert\cos\theta^*_{trk}\rvert < 0.85$	8.98	9.57	0.58
$N_{\text{extra}} < 3$	8.44	8.75	0.58
$E_{extra} < 0.400$ GeV	5.24	0.83	0.19
$N_{\pi^0} = 0$	4.74	0.66	0.19
$p^B_{\text{kaon}} > 1.1\,\text{GeV}/c$	4.14	0.25	0.19
$-0.85 < \cos\theta_{Pmiss} < 0.90$	4.14	0.25	0.19
ε_{sig}	$(30.2 \pm 2.4$ (stat) $)\%$	$(0.87 \pm 0.39)\%$	$(0.66 \pm 0.66)\%$

We reweight bin-by-bin the signal Monte Carlo so that it corresponds to the theoretical model and propagate the effect to the signal kaon momentum (bottom of Figure 31).

We find that ε_{sig} should be scaled by a factor of 96.6% . This factor is consistent with the number we get by doing the same operation on generic signal MC. There is a systematic error associated with the reweighting, discussed in section 9.

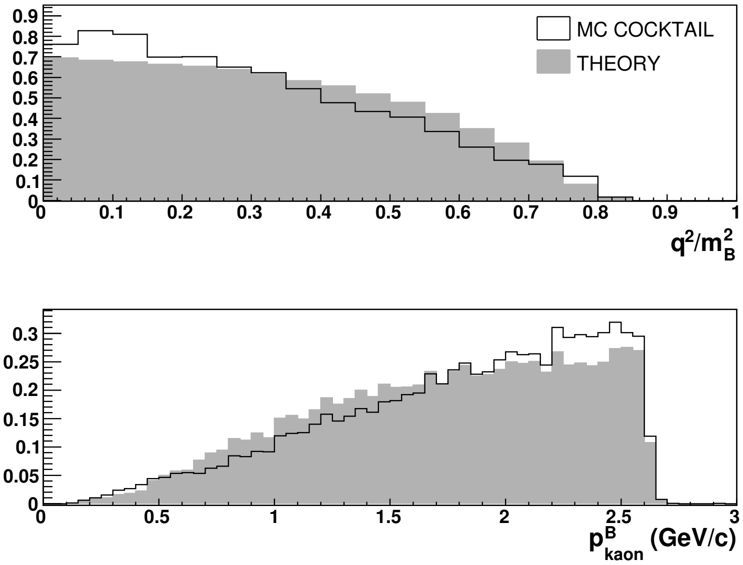

Figure 31: Top : Dilepton mass, relative to the mass of the B meson, for events with a B_{tag} and a good kaon candidate. Bottom : p^B_{kaon} distribution of kaon candidates for events with a B_{tag}. The two curves in each plot have equal area.

4.12 Kaon PID selection

In this analysis, the Kaon PID selection efficiency ϵ_{PID} measures the efficiency at identifying the hardest signal side track as a "tight" Kaon. It should be constant for generic and cocktail MC samples, so we can combine the statistics of the 3 samples and obtain a better value of the PID efficiency, which in turn will give a better value of $\varepsilon_{\mathrm{sig}}$.

We apply all the B_{tag} and B_{sig} selections except for the PID criteria, and we compare with the numbers we get when including the criteria. In other words, we do :

$$\epsilon_{PID} = \frac{\varepsilon_{\mathrm{sig}}(\text{without } K^{\pm} \text{ PID})}{\varepsilon_{\mathrm{sig}}(\text{with } K^{\pm} \text{ PID})} = 87.0\% \tag{6}$$

Without using the cocktail sample, we would get $\epsilon_{PID} = 0.838$. This induces a correction factor of 87.0% / 83.8% = 103.8 % to $\varepsilon_{\mathrm{sig}}$.

5 Total Efficiency

We define the total efficiency of reconstructing a signal event : $\varepsilon_{\rm tot} = \varepsilon_{\rm tag} \times \varepsilon_{\rm sig}$, with the tag yield correction applied on $\varepsilon_{\rm tag}$, the phase-space and the ϵ_{PID} corrections applied on $\varepsilon_{\rm sig}$, and we find that

$$\varepsilon_{\rm tot} = (0.244)\ \% \times 91.5\ \%\ ) \times (30.2)\ \% \times 96.6\% \ \times 1.038\%\ )$$
$$\boxed{\varepsilon_{\rm tot} = 0.0678\ \%}$$

This number is used in the calculation of the branching ratio.

6 Background Estimates

When the selection criteria described in section 4 are applied on generic Monte Carlo samples, we observe that the background is clearly dominated by B^+B^-, with only a small contribution from $B^0\overline{B}^0$ and none from $c\overline{c}$, uds or $\tau^+\tau^-$ (Tables 12 and 13). The contribution from charged B mesons is a mixture of peaking and combinatoric background.

Table 12: Effect of signal selection cuts on generic MC samples. Monte Carlo and offpeak data samples have been scaled to onpeak data luminosity.

	B^+B^-	$B^0\overline{B}^0$	$c\overline{c}$	uds	$\tau^+\tau^-$
B_{tag}	863875	250032	293644	262044	38.5
Kaon candidate	97576	9152	18827	14247	0.57
$\lvert\cos\theta^*_{trk}\rvert < 0.85$	90162	8434	17265	13000	0
$N_{\rm extra} < 3$	25271	1125	2962	2398	0
$E_{extra} < 0.400$ GeV	36.77	1.62	3.82	0.64	0
$N_{\pi^0} = 0$	26.27	0.81	1.27	0.64	0
$p^B_{\rm kaon} > 1.1\,{\rm GeV}/c$	12.76	0.20	0.63	0	0
$-0.85 < \cos\theta_{Pmiss} < 0.90$	12.38	0.20	0	0	0

6.1 Combinatoric and Continuum Backgrounds

Even if only a few combinatoric and no continuum background survive the B_{sig} selection, it could be a downward fluctuation due to low statistics.

The onpeak data in the $m_{\rm ES}$ sideband can be used as an alternative method to estimate the contribution from combinatoric and continuum backgrounds together : it has higher statistics and contains a negligible amount of signal events.

We first unblind the onpeak data in the sideband and count the number of events in that region. We then make the assumption that the full $m_{\rm ES}$ distribution is still well modelled by an Argus + Gaussian function, and, moreover, we assume that the Argus shape is stable when we apply the B_{sig} selection. This allows us to estimate the number of non-peaking events in the signal box, by using $R^{\rm areas} = 0.29 \pm 0.04$ (syst) as found in section 3.5. The $m_{\rm ES}$ distribution is shown in Figure 32 after all other selections have been applied. We stay blind to onpeak data in the $m_{\rm ES}$ signal box.

Table 13: Effect of signal selection cuts on generic MC samples and data. Monte Carlo samples have been scaled to onpeak data luminosity.

	Onpeak	All MC	OffPeak	Continuum
B_{tag}	1587590	1669634	541636	555726
Kaon candidate	147007	139803	33263	33075
$\|\cos\theta^*_{trk}\| < 0.85$	135498	128861	30592	30265
$N_{\text{extra}} < 3$	30888	31756	4556	5360
$E_{extra} < 0.400$ GeV	(*blind*)	42.8	9.7	4.4
$N_{\pi^0} = 0$	(*blind*)	29.1	9.7	1.94
$p^B_{\text{kaon}} > 1.1\,\text{GeV}/c$	(*blind*)	13.6	0	0.63
$-0.85 < \cos\theta_{Pmiss} < 0.90$	(*blind*)	12.6	0	0

This method is equivalent to fitting the onpeak m_{ES} sideband with 4 Argus function whose shape parameters were extracted from 4 different fits (see table 8), and then propagating these shapes in the signal box to estimate the number of non-peaking background there.

Table 14 compares the cumulative effect of the B_{sig} selection on the number of events in data, the m_{ES} sideband and how it propagates in the signal box (combinatoric events only) assuming a ratio of 0.29 ± 0.04 (syst) . The composition of the sideband is presented in table 15. We observe that the requirements on E_{extra} is more restrictive on MC events.

It is important to emphasize on the fact that this method of estimation uses the *data*, and avoids all the uncertainties due to discrepancies between real and simulated events.

We estimate that with 13 observed events in the sideband, there should be 3.77 ± 1.05 (stat) ± 0.15 (syst) events in the signal box due to combinatoric and continuum backgrounds.

Table 14: Effect of signal selection cuts on m_{ES} sideband in generic MC and data samples. Monte Carlo samples have been scaled to onpeak data luminosity. We assume a ratio of 0.29 ± 0.04 (syst) for R^{areas}. The number of non-peaking background is estimated from the data sideband.

	Onpeak	All MC	m_{ES} Sideband (data)	m_{ES} Sideband (MC)	Non-Peaking
B_{tag}	1587590	1669634	3 989 400	4 095 860	1 156 930
LHTKaon	147007	139803	225 658	199 098	65 441
$\cos\theta^*_{trk}$	135498	128861	207 630	183 212	60 213
N_{extra}	30888	31756	31 197	31 026	9 047
E_{extra}	(*blind*)	42.8	40	30.7	11.6
$N_{\pi^0} = 0$	(*blind*)	29.1	30	23.3	8.7
p^B_{kaon}	(*blind*)	13.6	14	8.2	4.0
$\cos\theta_{Pmiss}$	(*blind*)	12.6	13	7.69	3.77

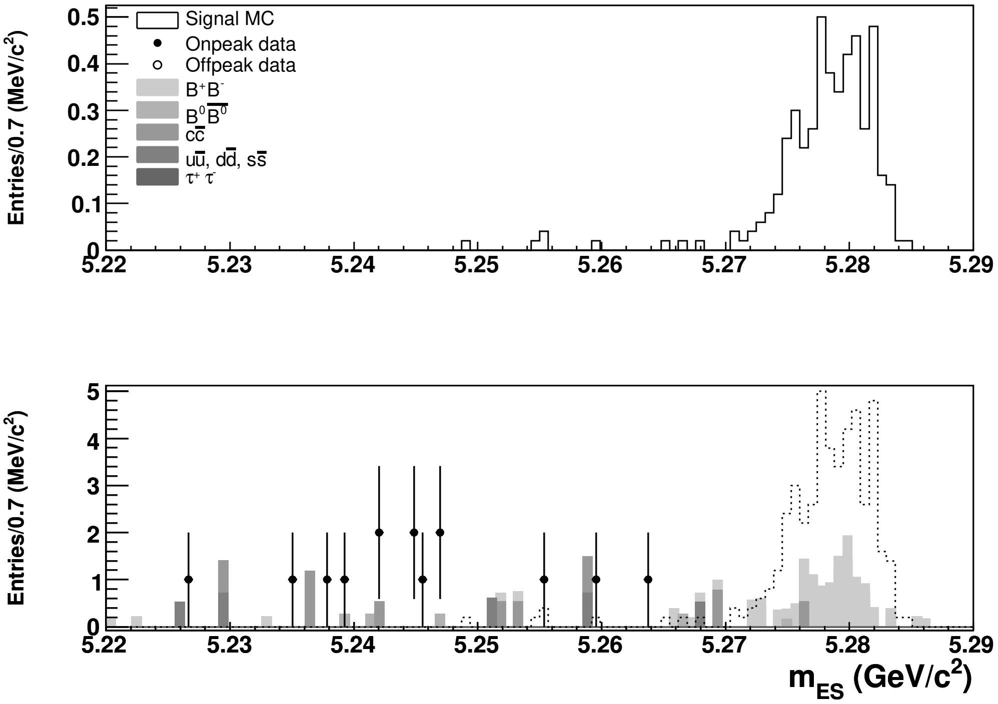

Figure 32: m_{ES} distribution after all other selections have been applied. Top : Signal Monte Carlo is scaled to $\mathcal{B}(B^+ \to K^+\nu\overline{\nu}) = 5.2 \times 10^{-5}$. Bottom : Offpeak data and generic Monte Carlo are scaled to onpeak data luminosity.

Table 15: Effect of consecutive signal selection on m_{ES} sideband in signal MC. $|\cos\theta_T| < 0.85$ and $Q_{\mathrm{tag}} = \pm 1$ are applied everywhere. MC samples has been scaled to onpeak data luminosity.

Criteria	B^+B^-	$B^0\overline{B}^0$	$c\overline{c}$	uds	$\tau^+\tau^-$
$Q_{\mathrm{tag}} = \pm 1$ & $\lvert\cos\theta_T\rvert < 0.85$	1245620	840082	1065570	944463	121
Kaon candidate	55554	24562	67430	51549	2.3
$\lvert\cos\theta^*_{trk}\rvert < 0.85$	51452	22716	61941	47102	1.7
$N_{\mathrm{extra}} < 3$	8917	2732	10664	8712	1.7
$E_{extra} < 0.400$ GeV	5.4	1.6	12.1	10.9	0.6
$N_{\pi^0} = 0$	2.8	1.4	10.8	7.7	0.6
$p^B_{\mathrm{kaon}} > 1.1\,\mathrm{GeV}/c$	0.6	0.6	3.8	2.6	0.6
$-0.85 < \cos\theta_{Pmiss} < 0.90$	0.6	0.6	3.8	1.9	0.6

6.2 Peaking Background

The number of B^+B^- background events found after applying the B_{sig} selection on generic MC samples is a combinaison of peaking and non-peaking events, and we must avoid double-counting the non-peaking, as it is already incorporated in the estimate of combinatorial background (see

Table 16).

Table 16: Different data types are used to estimate different backgrounds.

Data type	Background Type
Generic B^+B^-	Peak + Combinatorial
Onpeak data (sideband)	Continuum + Combinatorial

We find the non-peaking contribution using the same method as for data, by extrapolating the $m_{\rm ES}$ sideband in the signal box assuming the ratio of areas from various Argus shape. We found 3 events in the sideband, which translate into 0.563 ± 0.188 events after scaling to onpeak luminosity, and this propagates into 0.163 ± 0.055 events in the signal box using $R^{\rm areas}$ of $0.29{\pm}0.04$ (syst) .

This number must then be substracted from the 12.38 B^+B^- events found after applying the B_{sig} selection, and we estimate that 12.22 events from peaking background should be observed in generic B^+B^- samples.

Since this number is extracted exclusively from the peaking part, the (91.5 ± 0.8) % correction to $\varepsilon_{\rm tag}$ must be applied, as explained in section 3.5. We thus estimate the number of "real" peaking B^+B^- events in onpeak data to be 11.18 ± 1.40 (stat) ± 0.95 (syst) .

We note that the estimate of combinatorial background from data is consistent at the 3σ level with the estimate from B^+B^- combined with the $B^0\overline{B}^0$, but believe that the result from data is more reliable due to higher statistics.

When we add the contributions from the peaking and the combinatorial backgrounds, we obtain a total of 14.95 ± 1.75 (stat) ± 1.09 (syst) expected background.

6.3 Fake Signals

A particular source of background comes from topologically similar signals that survive all our selection cuts. Their maximum contribution is found by scaling the luminosity of the samples to the onpeak data using the last experimental upper limit. We found that the $B^+ \to K^{*+}\nu\overline{\nu}$ and $B^+ \to \pi^+\nu\overline{\nu}$ channels should contribute to the background at most by 0.23 ± 0.07 (stat) and 0.17 ± 0.17(stat) respectively, including the correction to the tagging yield efficiency. These must also be scaled down by the correction in the tag yield efficiency, and they are already counted in the estimate of peaking B^+B^- background.

7 Sidebands

Since we stay blind to onpeak data roughly after the requirement on E_{extra}, we can not compare directly the agreement between data and Monte Carlo samples after applying the last B_{sig} criteria. However, we can investigate the behavior indirectly by unblinding data in various sidebands. We make sure once again that each bin in each histogram has at least 10 times more onpeak data than the signal at the current upper limit (UL).

Different sideband have different particle content, which allows us to test the behavior of each background types almost independently, in an environment which is topologically similar to the $B^+ \to K^+\nu\overline{\nu}$ process. The different sidebands used in this analysis are :

- $5.225 < m_{\rm ES} < 5.265\,{\rm GeV}/c^2$
- $|\cos\theta_T| > 0.85$
- $p^B_{\rm kaon} < 0.5\,{\rm GeV}/c$
- $0.5 < E_{extra} < 1.5\,{\rm GeV}$
- Hardest track is not a LHTight Kaon

The $m_{\rm ES}$ sideband is used to explore both continuum and combinatoric backgrounds, the $\cos\theta_T$ sideband contains a lot of continuum events, while the last three are well populated with B^+B^- MC, hence are used to study peaking events.

In the following figures, we compare onpeak data to all generic MC samples, and offpeak data to generic uds + $c\overline{c}$ + $\tau^+\tau^-$ only. Since the size of the simulated continuum background sample is comparable to that on the onpeak data, the error bars (not shown) for MC sample should also be about the same size as those of the onpeak data.

7.1 Continuum Background

The E_{extra} distribution is plotted in the $\cos\theta_T$ and in the $m_{\rm ES}$ sidebands in Figures 33 and 34. The $p^B_{\rm kaon}$ spectrum has very low statistics in the $\cos\theta_T$ sideband, but it is shown in the $m_{\rm ES}$ sideband in Figure 35. We can also look at the $m_{\rm ES}$ distribution in the $\cos\theta_T$ sideband (Figure 36). We see from these plots that the two sidebands are dominated by continuum backgrounds, and that the generic MC samples seem to model well the physics of the data, especially in the signal region of the variable plotted. We expect that this agreement propagates in the signal box, or even improves, since the MC events are known to underestimate the data for $\cos\theta_T > 0.95$ (see Fig. 4).

7.2 $B\overline{B}$ Background

The $m_{\rm ES}$ distribution is presented in the $0.5 < E_{extra} < 1.5\,{\rm GeV}$ region, and for events in which the hardest track is not a kaon candidate (Figures 37 and 38). We see that the main contribution in the signal region comes from the peaking component of the B^+B^- background, and that there is a good agreement between data and MC samples. The tagging yield correction factor has not been applied here neither.

The momentum of the kaon candidate in these two sidebands is shown in Figure 39 and 40. A disgreement is observed for low momentum kaon, which should not propagate in the signal box.

Finally, the E_{extra} variable is shown in the $p^B_{\rm kaon} < 0.5\,{\rm GeV}/c$ region and for events in which the hardest track is not a kaon candidate, and we observe that there seem to be a small excess in data for high energy (Figures 41 and 42). The signal box of the E_{extra} variable, however, seems well modelled in both cases.

We thus conclude that the peaking component of the B^+B^- background is well modelled by data, so that the corresponding background estimate is reliable.

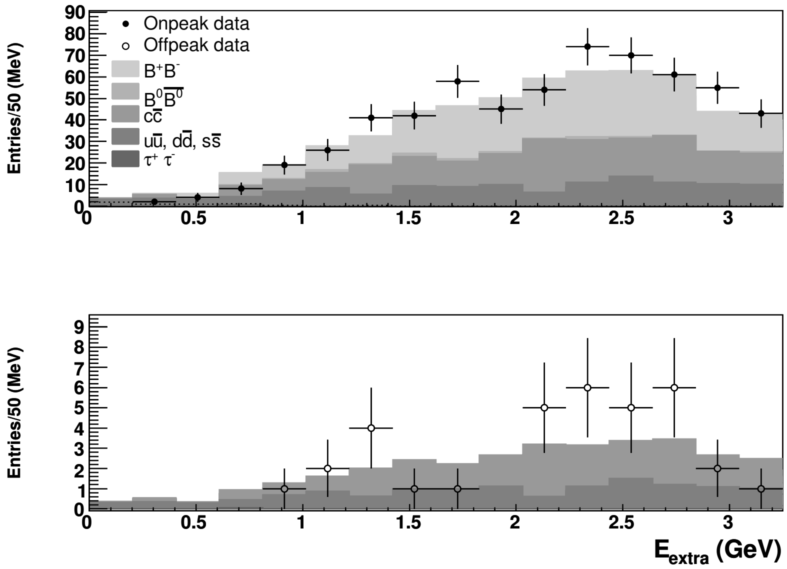

Figure 33: E_{extra} distribution in the $|\cos\theta_T| > 0.85$ sideband. Top : Offpeak data and generic Monte Carlo are scaled to onpeak data luminosity. Bottom : Generic $c\bar{c}$, uds and $\tau^+\tau^-$ Monte Carlo is scaled to offpeak data luminosity.

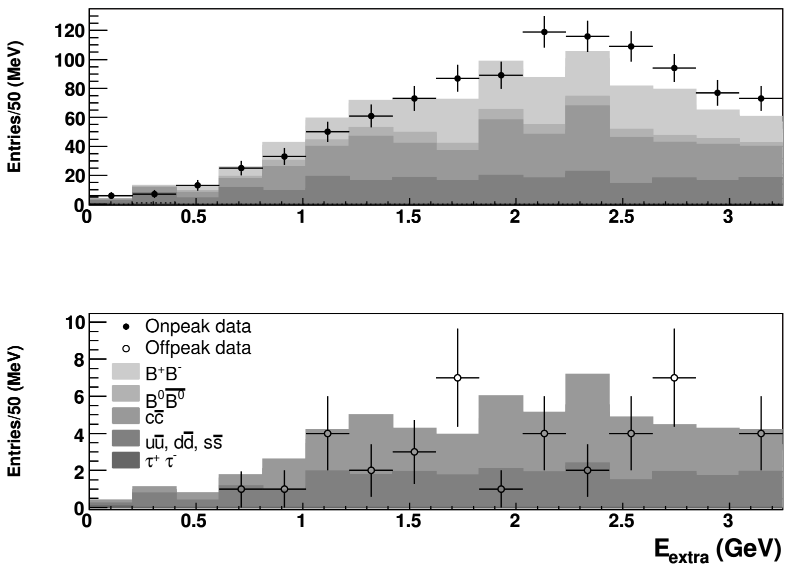

Figure 34: E_{extra} distribution in the $5.225 < m_{\mathrm{ES}} < 5.265\,\mathrm{GeV}/c^2$ sideband. Top : Offpeak data and generic Monte Carlo are scaled to onpeak data luminosity. Bottom : Generic $c\bar{c}$, uds and $\tau^+\tau^-$ Monte Carlo is scaled to offpeak data luminosity.

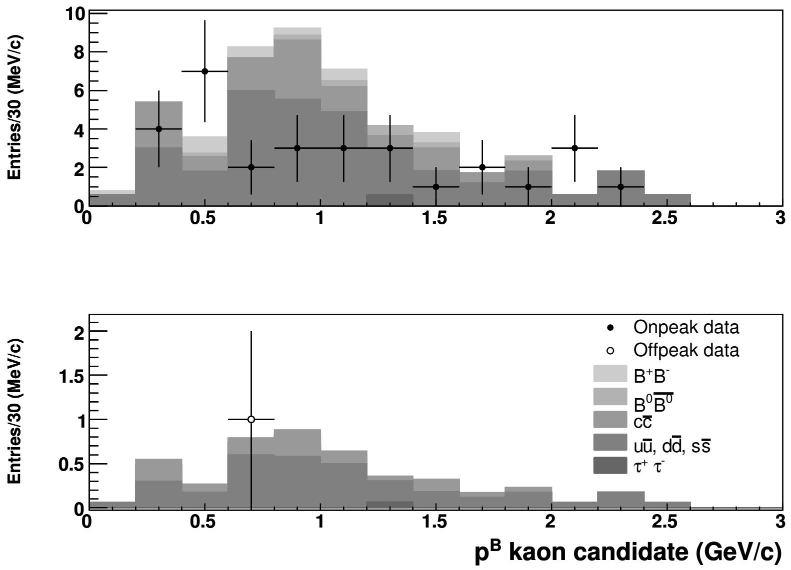

Figure 35: $p^B_{\rm kaon}$ distribution in the $5.225 < m_{\rm ES} < 5.265\,{\rm GeV}/c^2$ sideband. Top : Offpeak data and generic Monte Carlo are scaled to onpeak data luminosity. Bottom : Generic $c\overline{c}$, uds and $\tau^+\tau^-$ Monte Carlo is scaled to offpeak data luminosity.

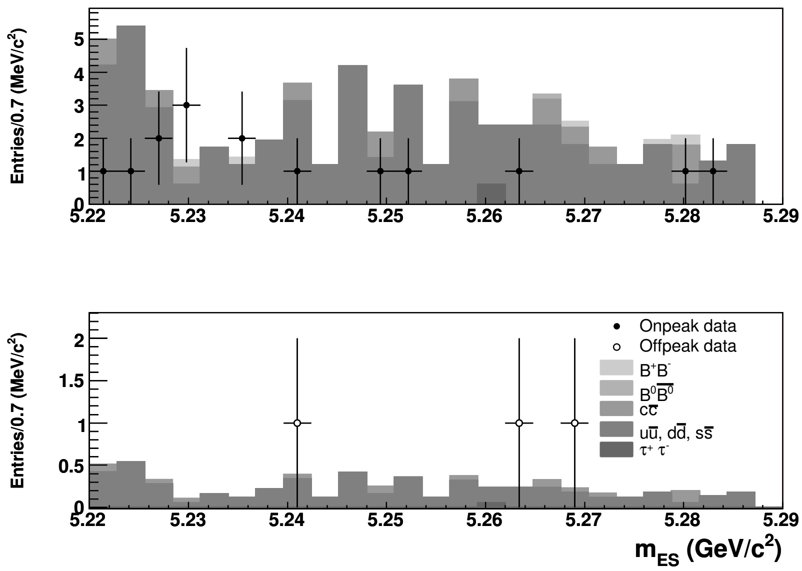

Figure 36: $m_{\rm ES}$ distribution in the $|\cos\theta_T| > 0.85$ sideband. Top : Offpeak data and generic Monte Carlo are scaled to onpeak data luminosity. Bottom : Generic $c\overline{c}$, uds and $\tau^+\tau^-$ Monte Carlo is scaled to offpeak data luminosity.

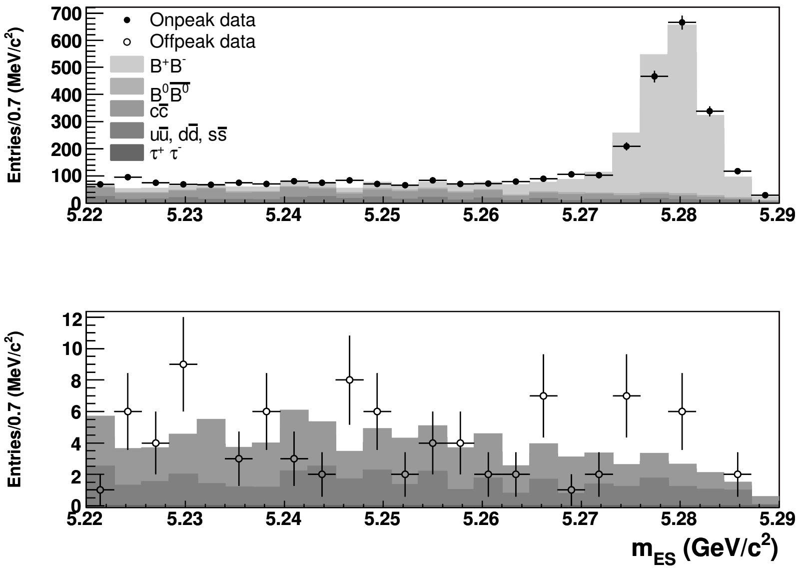

Figure 37: $m_{\rm ES}$ distribution in the $0.5 < E_{extra} < 1.5\,{\rm GeV}$ sideband. Top : Offpeak data and generic Monte Carlo are scaled to onpeak data luminosity. Bottom : Generic $c\overline{c}$, uds and $\tau^+\tau^-$ Monte Carlo is scaled to offpeak data luminosity.

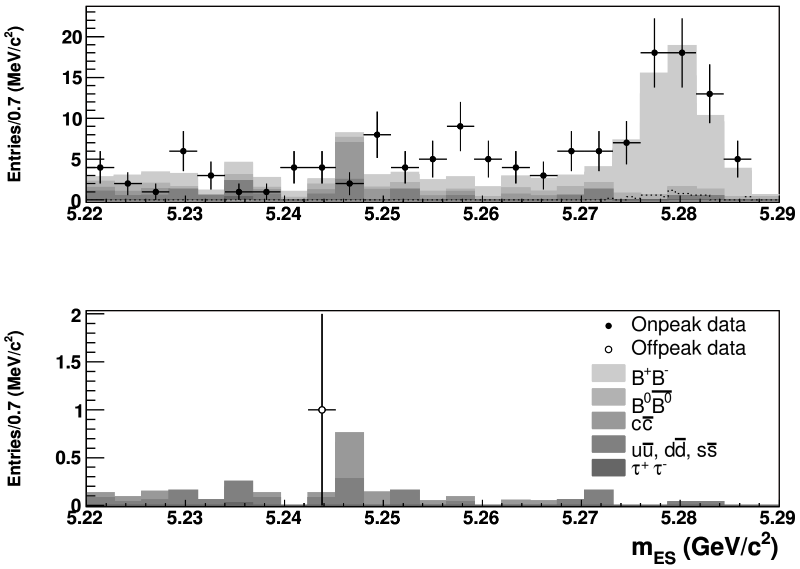

Figure 38: $m_{\rm ES}$ distribution for events in which the hardest track is not a kaon candidate. Top : Offpeak data and generic Monte Carlo are scaled to onpeak data luminosity. Bottom : Generic $c\overline{c}$, uds and $\tau^+\tau^-$ Monte Carlo is scaled to offpeak data luminosity.

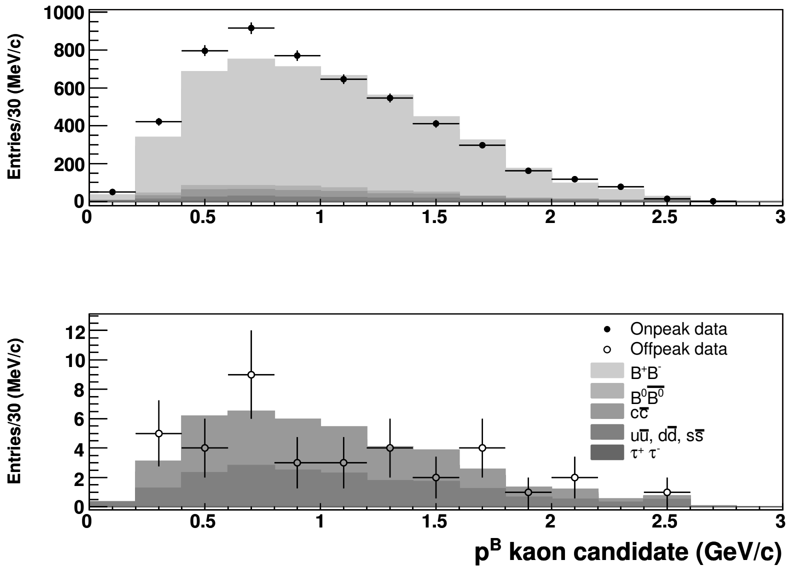

Figure 39: $p^B_{\rm kaon}$ distribution in the $0.5 < E_{extra} < 1.5\,$GeV sideband. Top : Offpeak data and generic Monte Carlo are scaled to onpeak data luminosity. Bottom : Generic $c\overline{c}$, uds and $\tau^+\tau^-$ Monte Carlo is scaled to offpeak data luminosity.

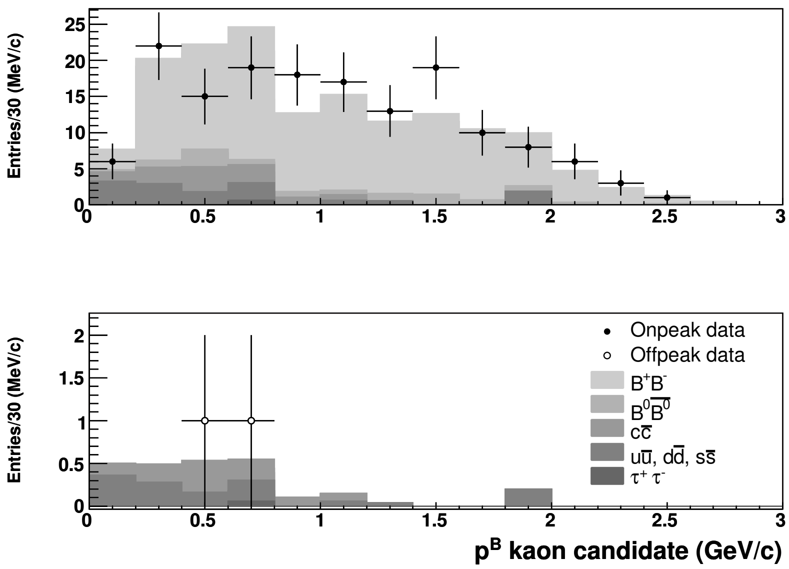

Figure 40: $p^B_{\rm kaon}$ distribution for events in which the hardest track is not a kaon candidate. Top : Offpeak data and generic Monte Carlo are scaled to onpeak data luminosity. Bottom : Generic $c\overline{c}$, uds and $\tau^+\tau^-$ Monte Carlo is scaled to offpeak data luminosity.

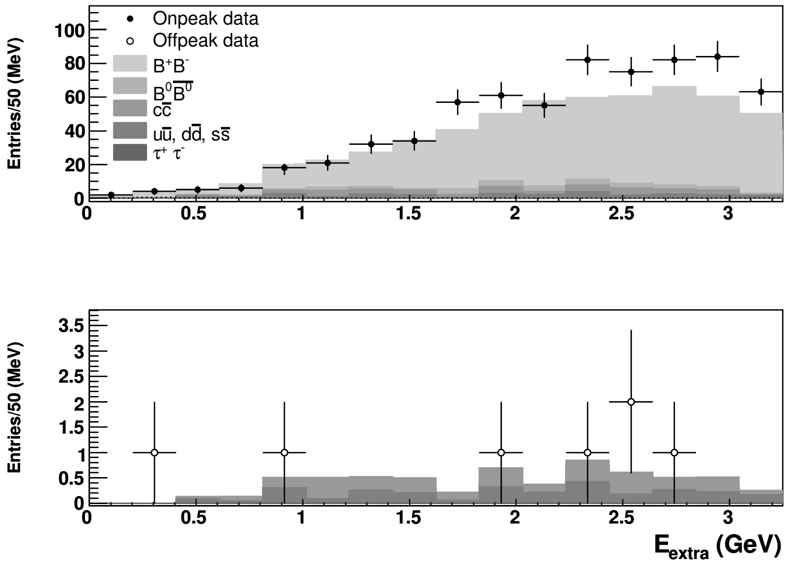

Figure 41: E_{extra} distribution in the $p^B_{\rm kaon} < 0.5\,{\rm GeV}/c$ sideband. Top : Offpeak data and generic Monte Carlo are scaled to onpeak data luminosity. Bottom : Generic $c\bar{c}$, uds and $\tau^+\tau^-$ Monte Carlo is scaled to offpeak data luminosity.

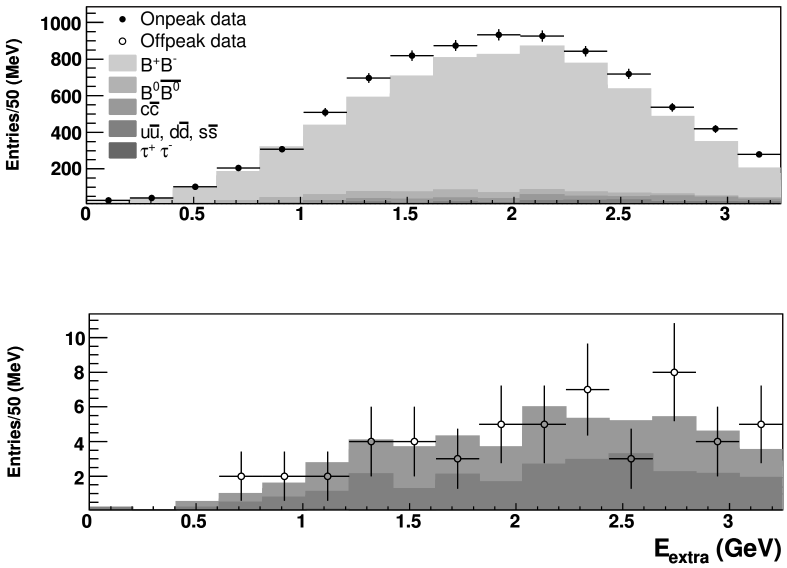

Figure 42: E_{extra} distribution for events in which the hardest track is not a kaon candidate. Top : Offpeak data and generic Monte Carlo are scaled to onpeak data luminosity. Bottom : Generic $c\bar{c}$, uds and $\tau^+\tau^-$ Monte Carlo is scaled to offpeak data luminosity.

8 Physics Results

The Branching ratio for the signal decay $B^+ \to K^+\nu\overline{\nu}$ is given by

$$\mathcal{B}(B^+ \to K^+\nu\overline{\nu}) = \frac{N_{sel} - N_{bg}}{2 \times N_{B^+B^-} \times \varepsilon_{\rm tot}} \tag{7}$$

where N_{sel} is the number of data events selected after all the requirements have been applied, N_{bg} is the estimated number of background events in the signal box, $N_{B^+B^-}$ is the number of B^+B^- pairs produced in Runs 1 to 4 onpeak data, and $\varepsilon_{\rm tot}$ is the total signal efficiency. The value of $\varepsilon_{\rm tot}$ was entirely derived from signal Monte Carlo simulations, the number of B^+B^- pairs was given by the *BABAR* Data Quality Group, N_{bg} was estimated using generic MC samples for the peaking component part, and data for the continuum and combinatoric contributions to the background. These values are listed in Table 17, and were used in the calculation of the UL using the `syslimit` calculator [19]. The sensitivity S_K in this context is defined as $S_K = N_{B^\pm} \times \varepsilon_{\rm tot}$. The systematic error used in this calculation is treated in the next section. The upper limits corresponding to various N_{sel} are presented in Table 18, calculated at the 90% confidence level (CL). Previous results on this process are shown in Table 19 for *BABAR* [17], BELLE [22] and CLEO [23] collaborations.

Table 17: Values used to compute an upper limit on the Branching ratio for the process $B^+ \to K^+\nu\overline{\nu}$. The first uncertainty is statistical, the second is systematic.

$\sigma_{B^+B^-}$	0.525
$\mathcal{L}$	$208.73\,\mathrm{fb}^{-1}$
$N_{B^\pm}$	$(229.953 \pm 1.473) \times 10^6$
$\varepsilon_{\rm tot}$	$(0.0678 \pm 0.0043$ (stat) $)\%$
N_{bg}	14.95 ± 1.75 (stat) ± 1.09 (syst)
N_{sel}	???±???±???
S_K	150804 ± 25129

Table 18: Upper limits (UL) on the Branching ratio for the process $B^+ \to K^+\nu\overline{\nu}$ using the Cousins-Highland method at a 90% confidence level (CL).

N_{sel}	UL ($\times 10^{-5}$)
10	0.73
11	1.50
12	2.27
13	3.02
14	3.78
15	4.54
16	5.29
17	6.07
18	6.84
19	7.60
20	8.38

Table 19: Previous results for the process $B^+ \to K^+\nu\overline{\nu}$. All UL on $\mathcal{B}$are calculated at a 90% CL.

Collaboration	$\mathcal{B}$	data set (fb^{-1})
BABAR with hadronic tags only	$< 6.7 \times 10^{-5}$	80.06
BABAR with semi-leptonic tags only	$< 7.0 \times 10^{-5}$	80.06
BABAR with both hadronic and semi-leptonic tags	$< 5.2 \times 10^{-5}$	82.00
BELLE	$< 3.6 \times 10^{-5}$	253.00
CLEO	$< 6.1 \times 10^{-4}$	9.24
PDG	$< 2.4 \times 10^{-4}$	
Standard Model	$3.8^{+0.12}_{-0.06} \times 10^{-6}$	-

9 Systematic Uncertainties

The 90% CL upper limit we extract for the $B^+ \to K^+\nu\overline{\nu}$ process depends on the systematic uncertainty associated with the quantities involved in the calculation.

We defined earlier $\varepsilon_{\text{tot}} = \varepsilon_{\text{tag}} \times \varepsilon_{\text{sig}}$, so we study the uncertainties related to the composite quantities, then propagate the error to ε_{tot}. We also estimate the systematic uncertainty on the number of background events, for the peaking and non-peaking components separately.

9.1 Uncertainty on ε_{tag}

The possible uncertainties associated with ε_{tag} come from :

- the observed shape of the m_{ES} peak
- the tag yield correction factor

In this analysis, the global shape of the peak is slightly different in MC and data events (see Figure 10). Since the m_{ES} window is wide enough, the shift in the peak affects only events which are 3σ away. Moreover, we correct for the tagging yield, so the overall shape has a negligible impact on the value of ε_{tag}.

The second source is studied by varing the shape of the Argus fit (i.e. by using different sets of parameters to model the Argus) and by comparing the correction factor obtained using different functions. We obtain an uncertainty of 0.8 % on the 91.5 % correction factor, which translates in an uncertainty of 0.002 % on ε_{tag}. This method assumes that continuum and combinatoric backgrounds are modelled correctly by an Argus function in nature, which is uncertain. We believe that a 5 % uncertainty on the correction factor is more realistic (inducing a 0.011% uncertainty on ε_{tag})

There is an uncertainty on the exact onpeak data luminosity and on the $B\overline{B}$ cross-section, but when we scale the MC tagging yield to the data, we implicitely correct for these two uncertainties.

9.2 Uncertainty on ε_{sig}

The uncertainty associated with ε_{sig} has the following sources :

- Tracking efficiency
- Kaon selection and PID
- Bump in $\cos\theta^*_{trk}$ near +1
- Discrepancy in N_{extra}
- Discrepancy in E_{extra}
- Discrepancy in π^0 multiplicity
- Discrepancy in the spectrum of p^B_{kaon}
- Decay model used to compute p^B_{kaon}

The systematic uncertainty associated with the tracking efficiency (1.2%/trk) and with the kaon selector (1.1%/`LHTightKaon`) are recipies given by the *BABAR* tracking "taskforce" and the PID group ([20] and [21]) respectively. The former is a result from an unperfect tracking algorithm, combined with systematic uncertainty at measuring hits in the DCH and EMC ; the latter takes into account the uncertainty of a dE/dX measurement, as well as the uncertainty in measuring the Cherenkov angle in the DIRC. It is valid only in the high momentum regime, which is the case in this analysis.

We recall that tagged signal events have on average 2.74 tracks per event, but this number drops to 1.13 after all cuts have been applied. Only one of these tracks is required to pass the kaon PID criteria. The latter is more restrictive on MC than on data samples by about 1%, which translates into a systematic uncertainty of 0.40% .

The bump in $\cos\theta^*_{trk}$ result in an over-estimate of about 3000 generic B^+B^- MC events in that region. However, these events seem to behave normally in all other distributions, as we do not see distinct discrepancies that could be associated with them. Hence we treat them as normal events, and since the efficiency of that criteria is exactly the same in generic MC and in data events, it does not contribute to any uncertainty.

The error from the discrepancy in π^0 multiplicity is evaluated by looking at the distribution of N_{π^0} in figure 26, and finding the difference in the selection efficiencies for data (20.8 %) and MC (18.8 %) samples. This difference of 2.0 % results in a 0.67% uncertainty on the signal efficiency.

Generic MC (data) tagged events have 6.25 (6.58) extra tracks with momentum 306 (329) MeV/c on average (see Figures 17 and 19), and 12.7 (11.2) clusters of energy 28 (40) MeV on average (see Figures 22 and 23). When we combine these two effects into E_{extra}, every simulated event should be weighted up by 0.33 tracks, and weighted down by 1.5 clusters on average. We evaluate the impact of this by correcting for these amounts in every signal MC events, and by re-evaluating $\varepsilon_{\mathrm{sig}}$. This results in an uncertainty of 3.40% .

However, the E_{extra} distributions in the four sidebands seem to show a good agreement in the signal region, hence it seems that the actual uncertainty should be somewhat smaller than that, and will be investigated in the final version of this document.

We estimate the uncertainty related to the reweighting of the phase-space model by comparing the values of $\varepsilon_{\mathrm{sig}}$ obtained when reweighting the q^2 spectrum to the 1σ curves in the dynamical model [11]. It results in an uncertainty of 0.39% .

The impact of the discrepancy in the p^B_{kaon} distribution can be studied by looking at the same distribution but for events in which the hardest track is not a kaon, or for events with kaon but in the E_{extra} sideband (Figures 40 and 39). We observe a good MC-data agreement in the $p^B_{\mathrm{kaon}} > 1.1\,\mathrm{GeV}/c$ region in both figures. Since events with low E_{extra} mostly have a high p^B_{kaon}, and since the E_{extra} variable seems well modeled in the low energy regime, we conclude that the p^B_{kaon} variable should be also well modeled, hence we assign no systematic error.

9.3 Uncertainty on N_{bg}

Appart from the uncertainty due to the phase-space model, all the sources of uncertainty on $\varepsilon_{\mathrm{tag}}$ and $\varepsilon_{\mathrm{sig}}$ also apply on the number of peaking background and are estimated using the same arguments.

For the combinatorial background, there is only one uncertainty, coming from the propagation of Argus functions. The systematic error on the ratio of the sideband/signal box areas is found by looking at the variation on the ratio when using different Argus shapes, as explained in section 3.5. To illustrate this method, let's consider the extreme case : approximate the Argus as a rectangle, in which case the ratio would be 0.45. We obtain the value of 0.29 ± 0.04 (syst) that is more realistic, and the 4 % uncertainty on that ratio produces a 0.52 uncertainty on N_{bg}.

Table 20 presents the complete treatment of statistical and systematic uncertainty, and we obtain that the total error on $\varepsilon_{\mathrm{tot}}$ and on N_{bg} are 0.0088 % and 1.09 .

Table 20: Statistical and systematic uncertainties.

Quantity	Source	value	± stat	± syst
$\varepsilon_{\mathrm{tag}}$		0.224 %		
	Statistics		0.006%	
	Tag Yield Correction			0.011%
$\varepsilon_{\mathrm{sig}}$		30.3 %		
	Statistics		2.29%	
	Tracking Efficiency			0.41%
	PID Efficiency			0.33%
	Kaon Selection			0.40%
	N_{π^0} Dicrepancy			0.67%
	E_{extra}			3.40%
	Decay Model			0.39%
	Total Systematic			3.55%
$\varepsilon_{\mathrm{tot}}$ (%)		0.0678 %	0.0043	0.0088
Peaking		11.18		
Background	Statistics		1.40	
	Tag Yield Correction			0.56
	Tracking Efficiency			0.18
	PID Efficiency			0.12
	N_{π^0} Dicrepancy			0.22
	E_{extra}			0.70
	Total Systematic			0.95
Combinatorial		3.77		
Background	Statistics		1.05	
	Argus Shape			0.52
N_{bg}		14.95	1.75	1.09

9.4 Peaking B^+B^-

In this analysis, we deal with the extra yield in the peaking B^+B^- generic MC sample by scaling down the overall B^+B^- contribution in every calculations we make. However, this assumes that the "extra" B^+B^- events spread uniformly in most distributions. It could be possible that these extra events have special dynamics, and would behave differently from normal B^+B^- events.

Here we compile the places where MC-data discrepancies seem to be caused by an overestimations of B^+B^- (where offpeak data agrees well with $c\overline{c}$ + uds + $\tau^+\tau^-$). We do not attempt to prove that there is a correlation between the candidates in these regions and the overestimation of B^+B^- under the m_{ES} peak. This is left for future work.

These regions are :

- R2All between 0.15 and 0.4
- $\cos\theta_B$ between -0.5 and 0.9
- $\cos\theta^*_{trk}$ between 0.7 and 0.9
- p^B_{kaon} between 0.7 and 1.8 GeV/c
- Total cluster energy between 0.2 and 1.0 GeV
- $\cos\theta_{Pmiss}$ between 0.85 and 1.0

10 Summary

We use hadronic B tags, reconstructed with the semi-exclusive method, and search in the decay of the other B mesons for the signal process $B^+ \to K^+\nu\overline{\nu}$. We estimate that 14.95 ± 1.75 (stat) ± 1.09 (syst) background events should show up in the signal box after all the selection criteria are applied. After unblinding, we observe ???±???±??? events in onpeak data, from which we set an upper limit of $\mathcal{B}(B^+ \to K^+\nu\overline{\nu}) <???? \times 10^{-5}$, at 90 % CL.

11 Aknowledgements

We would like to thank Steven Robertson for his detailed explanation of the previous analysis, Miika Klemetti for sharing his root macros, and David Côté for his help in writing the code for "truth-matching".

References

[1] A. J. Buras, M. Spranger and A. Weilner, "The Impact of Universal Extra Dimensions on the Unitarity Triangle and Rare K and B Decays", hep-ph/0212143.

[2] T. Barakat, "Rare $B^+ \to K^{*+}\nu\overline{\nu}$ decay with polarized K^* in the fourth generation model", hep-ph/0106296.

[3] B. Holdom and M. V. Ramana, "New flavor physics in b decays", hep-ph 9509272.

[4] G. Buchalla, G. Burdman, C. T Hill and D. Kominis, "GIM Violation and New Dynamics of the Third Generation", hep-ph/9510376.

[5] Z. Xiao and L. Yao, "Rare decay $B \to X_s\nu\overline{\nu}$ in the two-Higgs-doublet model of type-III", hep-ph/0212008.

[6] D. Melikhov, N. Nikitin and S. Simula, "Right-handed currents in rare exclusive $B^+ \to K^{(*)+}\nu\overline{\nu}$ decays", hep-ph/9803269.

[7] C. S. Kim, Y. G. Kim and T. Morozumi, "New Physics Effects in $B^+ \to K^{(*)+}\nu\overline{\nu}$ Decays", hep-ph/9905528.

[8] C. Bobeth, A. Buras, F. Krüger and J. Urban, "QCD Corrections to $B \to X_{d,s}\nu\overline{\nu}$, $B^0 \to \ell^+\ell^-$, $K^+ \to \pi^+\nu\overline{\nu}$ and $K_L^0 \to \mu^+\mu^-$ in the MSSM", hep-ph/0112305.

[9] A. J. Buras, "Flavour Physics : CP violation and rare Decays", hep-ph/0101336.

[10] ALEPH collaboration, Eur. Phys. J. **C19** 213-227, 2001: hep-ex/0010022.

[11] G. Buchalla, G. Hiller and G. Isidori, "Phenomenology of non-standard Z couplings in exclusive semileptonic $b \to s$ transitions", Phys. Rev. **D63** 014015 (2001): hep-ph/0006136.

[12] C. Bird, R. Kowalewski and M. Pospelov, "Dark Matter pair-production in $b \to s$ transitions", Mod. Phys. Lett. A, (2006) XXXXX.

[13] A. J. Buras, "Weak Hamiltonian, CP Violation and Rare Decays", hep-ph/9806471.

[14] S. Godfrey and N. Isgur, Phys. Rev. **D32**, (1985) 189.

[15] Particle Data Group, D. E. Groom *et al.*, Eur. Phys. Jour. C **15** 1 (2004).

[16] G. C. Fox and S. Wolfram, Phys. Rev. Lett., **41** 1581 (1978).

[17] *BABAR* collaboration, *BABAR*-CONF-04/50, 2005: hep-ex/0408086.

[18] D. del Re *et al.*, "Semi-Exclusive B Reconstruction" *BABAR* Analysis Document #271.

[19] *BABAR* collaboration, "syslimit 1.0" program, `http://www.slac.stanford.edu/~barlow/syslimit.html`.

[20] `http://www.slac.stanford.edu/BFROOT/www/Physics/TrackEfficTaskForce /TrackingTaskForce-2004.html`

[21] S. Spanier and G. Mancinelli, "Kaon Identification in the *BaBar* Experiment ", *BaBar* Analysis Document #116.

[22] BELLE collaboration, BELLE-CONF-0566, 2005: hep-ex/0507034.

[23] CLEO collaboration, "SEARCH FOR THE RARE DECAY OF A B MESON TO A K MESON AND TWO NEUTRINOS", 2004 `http://hdl.handle.net/1813/92`